Connection between South Mediterranean climate and North African atmospheric circulation during the last 50,000 yr BP North Atlantic cold events

Viviane Bout-roumazeilles, N Combourieu Nebout, O Peyron, E Cortijo, A Landais, Valérie Masson-Delmotte

Connection between South Mediterranean climate and North African atmospheric circulation during the last 50,000 yr BP North Atlantic cold events

V. Bout-Roumazeilles[a,*], N. Combourieu Nebout[b], O. Peyron[c], E. Cortijo[b], A. Landais[d], V. Masson-Delmotte[d]

[a]UMR CNRS 8110, Processus et Bilans des Domaines Sédimentaires, Universitéde Lille 1, 59655 Villeneuve d'Ascq Cedex, France

[b]UMR CEA-CNRS 1572, Laboratoire des Sciences du Climat et de l'Environnement, Domaine du CNRS, 91198 Gif-sur-Yvette, France

[c]UMR CNRS 6565, Laboratoire de Chrono-écologie, Universitéde Franche-Comté, 16 Route de Gray, 25030 Besançon, France

[d]IPSL/CEA-CNRS-UVSQ, Laboratoire des Sciences du Climat et de l'Environnement, CEA Saclay, l'Orme des Merisiers, 91191 Gif-sur-Yvette Cedex, France

[*]Corresponding author. Tel.: +33320434395; fax: +33320434910.

E-mail address: viviane.bout@univ-lille1.fr (V. Bout-Roumazeilles).

Abstract

High-resolution clay mineralogical analyses were performed on sediment deposited during the last 50,000 yr in the Alboran sea (ODP Site 976). The clay mineral record is compared with pollen assemblages and with annual precipitation (Pann) and mean temperatures of the coldest month (MTCO) reconstructed with the modern analog technique (MAT). Enhanced contribution of palygorskite, a typical wind-blown clay mineral, characterizes the North Atlantic cold climatic events. Coeval development of the semi-arid vegetation (*Artemisia* rich) associated with a drastic fall of reconstructed precipitations and temperatures, suggest cold and arid continental conditions in the West Mediterranean area during North Atlantic cold events. The clay mineral association, especially the palygorskite content and the illite-to-kaolinite ratio, indicate western Morocco as one of the major source of the clay-size fraction during the North Atlantic cold events. The maximum abundance of *Artemisia* associated with the presence of *Argania* pollen both indicate Morocco as the main origin for pollen during these cold periods. The comparison of these pollen and clay mineral-specific features allows us to pinpoint western Morocco as the dominant source of wind-

blown particles during North Atlantic cold events. These specific mineralogical composition and palynological assemblages reveal enhanced aridity over North Africa and intensification of winds favouring dust erosion and transport from North Africa toward the Alboran Sea during the North Atlantic cold events. According to atmospheric models, such a meridian transport (1) likely results from the development of strong and stable anticyclonic conditions over the tropical Atlantic and North Africa, similar to today's summer meteorological configuration and (2) implies a northward position of the westerly winds during North Atlantic cold events. Finally the synoptic situation over the West Mediterranean during the North Atlantic cold events is compared with the North Atlantic Oscillation (NAO), suggesting that during the cold Atlantic events, weather regimes over Europe and North Africa may have been systematically shifted towards a positive NAO situation.

1. Introduction

The Alboran Sea is a semi-enclosed basin situated in a climatic transitional area between the Atlantic Ocean and the Mediterranean Sea (Fig. 1). In the Mediterranean Sea, the formation of deep-water is mainly driven by seasonal climatic conditions: summer anticyclonic conditions favor evaporation over precipitation and dense water mass formation (Béthoux, 1980). Moreover, the displacement of European depressions over the Mediterranean creates high climatic instability and allows frequent incursions of the westerly winds. These climatic changes strongly influence the Alboran sea sedimentation: several high-resolution records reveal a millennial climate variability similar to the Dansgaard–Oeschger events defined in Greenland ice cores (Cacho et al., 2000; Moreno et al., 2002, 2005; Sánchez-Goñi et al., 2002; Combourieu Nebout et al., 2002). The more intense cold stadials favored the northern continental ice-sheet growth, which provoked ice-calving and major iceberg discharges in the North Atlantic ocean. These so-called Heinrich events (HE) are recorded in sediments by the abundance of coarse-grain detritus associated with a typical fresh meltwater supply. Isotopic records indicate that deep convection was more efficient during cold stadials and HE than during warm interstadials suggesting an intensification of the northwesterlies during North Atlantic cold climatic events (Cacho et al., 2000). Pollen analyses reveal that arid and cold conditions develop on the surrounding continents during the HE and some cold stadials (Combourieu Nebout et al., 2002; Sánchez-Goñi et al., 2002). Moreover, grain-size and elemental analyses also suggest enhanced eolian contribution to the Alboran sedimentation during North Atlantic cold events (Moreno et al., 2002, 2005). The

occurrence of such climatic conditions over the Mediterranean seems to be linked to the westerly regime over Europe and very similar to weather regime variations which characterize the North Atlantic Oscillation (NAO) (Rohling et al., 1998; Cacho et al., 2000; Combourieu Nebout et al., 2002; Sánchez-Goñi et al., 2002; Moreno et al., 2005). Mechanisms, however, are still unclear. In order to understand the links between the cold climatic events recorded in Greenland ice core (Johnsen et al., 1992) and the climatic changes over the Mediterranean area and North Africa, high-resolution mineralogical analyses of sediments from the ODP Site 976 (36112N, 4118W) were performed on the 0–50 ka interval. Indeed previous studies in the tropical Atlantic Ocean demonstrated that mineralogy could successfully be used to trace the source and transport of wind-blown particles (Caquineau et al., 1998). Our main objective is then to trace the variations of dust emission and transport over North Africa and South-West Mediterranean related to the North Atlantic Marine Isotopic Stage 3 cold events (Dansgaard–Oeschger stadials and HE). The composition of the clay mineral fraction is also compared to pollen assemblages in order to reconstruct the western Mediterranean oceanic and continental paleoenvironments and climate changes during the last 50,000 yr BP.

2. Eolian input, atmospheric scenario and clay mineral transport

The eolian supply contributes significantly to the terrigenous marine sedimentation and can then be used to trace the climatic evolution of continental areas (Sarnthein et al., 1982; Ruddiman et al., 1989). But the dust transport shows strong seasonal variability in occurrence, origin, trajectories and composition (Prospero et al., 1981; Pye, 1987; Chiapello et al., 1997; Moulin et al., 1997; Grousset et al., 1998; Ratmeyer et al., 1999).

2.1. Eolian and riverine contribution to deep-sea sediments

Sedimentation in the Mediterranean Sea is mainly terrigenous due to the vicinity of the surrounding continents associated with important riverine and eolian supplies. At present-day a major part of detrital clays is supplied via rivers (Milliman and Meade, 1983; Stanley et al., 1992). In the eastern Mediterranean, most particles (120.106 t/yr) are provided by the Nile River. The Rhone River with an annual discharge of 31.106 t/yr is the main contributor to sedimentation in the northwestern Mediterranean whereas the Po River (13.106 t/yr) and the Ebro River (18.106 t/yr) are of minor influence.

The eolian contribution to deep-sea sediments has been demonstrated in several studies (Prospero, 1981a, b; Pye, 1987) especially in Mediterranean fine-grained fraction (Tomadin and Lenaz, 1989; Matthewson et al., 1995; Guerzoni and Chester, 1996). Because mineral aerosols can be long-range transported (Rea et al., 1985; Guerzoni and Chester, 1996), massive plumes of desert dust are exported to the Atlantic Ocean and to the Mediterranean all year long. There is still a debate about the atmospheric contribution to deep-sea sediments with estimations ranging from 10% to 50% (Loye-Pilot et al., 1986; Guerzoni et al., 1997). In fact, the eolian supply is generally estimated to be one order of magnitude lower than fluvial supply at the scale of the whole Mediterranean basin (3.9.106 t/yr) (Bergametti et al., 1989c). This value probably underestimates the real contribution of eolian supply since an important part of river material may be trapped on the continental shelf on the West Mediterranean (Sarnthein et al., 1982; Ratmeyer et al., 1999). Previous studies based on radionucleides (Gascó et al., 2002) and trace metal budget (Elbaz-Poulichet et al., 2001) concluded that sedimentation in the western Mediterranean and in the Alboran Sea is significantly fed by eolian particles compared to riverine inputs. This characteristic results both from a rather low fluvial discharge from the Ebro River compared to other peri-Mediterranean rivers and from extended desert areas (Sahara and Sahel) seasonally exposed to strong winds, which provide huge amounts of dust particles to the atmosphere (Prospero, 1981a; Coudé-Gaussen, 1982; Middleton, 1985; Pye, 1987).

2.2. Dust origin

Arid regions such as the Sahara and semi-arid regions such as northern North Africa or Sahel provide dust particles to the Atlantic Ocean and the Mediterranean Sea (Prospero et al., 1981; Coudé-Gaussen, 1982; Matthewson et al., 1995). Grain-size analyses of wind-blown dust reveal two populations characterizing different source areas and transport mechanisms. Although major dust emission are generally situated in the subtropical desert belt and in semiarid regions (Pye, 1987; Chamley, 1989 and references therein), grain-size distribution reveals that the coarsest fraction is remobilized from Saharan dunes whereas the finer size fraction originates from paleosols and little consolidated formations located on the southern and northern borders of the desert (Rognon et al., 1996). The largest particles are typical of dust storm and are generally transported by trade winds below 100km of altitude, being restricted to continental and adjacent marine areas (Torres- Padrón et al., 2002). By contrast, the fine-grained particles (o2 mm) move over long distances as high-altitude

aerosols (Schu¨tz, 1980). Finally satellite-derived data as Infrared Dust Differencing Index (IDDI) and Total Ozone Mapping Spectrometer (TOMS) suggest that the Bodélédepression in Chad (Brooks and Legrand, 2000; Washington and Todd, 2005) and West Sahara and more generally topographic lows are among the most present-day dust productive areas.

2.3. Wind systems

The modern atmospheric circulation (Fig. 1) over North Africa is mainly controlled by the northeast trade winds (TW) and by the mid-tropospheric Saharan Air Layer (SAL) (Grousset et al., 1992; Matthewson et al., 1995). The resulting southern Saharan winds are mono-directional with a general westward transport. The dust plume extension is seasonally modulated by the migration of the Inter-Tropical Convergence Zone (ITCZ) (Prospero et al., 1981; Pye, 1987; Torres-Padrón et al., 2002). In winter, when the ITCZ occupies its southernmost position at 81N (Prospero et al., 1981; Pye, 1987), Saharan dust originates from southern Sahara and Sahelian regions and is transported toward the tropical Atlantic Ocean by the northeast trade winds (Schütz, 1980; Coudé-Gaussen et al., 1987; Bergametti et al., 1989b; Grousset et al., 1992, 1998; Matthewson et al., 1995; Chiapello et al., 1995, 1997; Moulin et al., 1997). In summer, trade winds are geographically restricted due to the northern migration of the ITCZ (201N). Intensive insolation over Sahara creates strong surface winds and large-scale convection which lifts particles to the high atmosphere (5 km). Particles originating from western and central part of the Sahara (e.g. Torres-Padrón et al., 2002) are transported at high-altitude by the SAL (Fig. 1), above the trade wind inversion toward the tropical Atlantic (Schütz, 1980; Coudé-Gaussen et al., 1987). A north-turning part of the SAL moves (NSAL) into an anticyclonic gyre along the African coast (Fig. 1) and reaches the Mediterranean (Prospero et al., 1981; Bergametti et al., 1989b).

By contrast, winds (Fig. 1) are pluri-directionnal in northern Sahara (Coudé-Gaussen et al., 1982). Their trajectories depend on the relative position of both high and low-pressure systems over the Atlantic Ocean, the Mediterranean and on the westerly wind regime over Europe (Coudé-Gaussen et al., 1982; Bergametti et al., 1989c; Moulin et al., 1997; Rodríguez et al., 2001). Dust transport is sporadic in nature but a single event can account for more than 50% of the annual eolian flux (Guerzoni et al., 1997). Such meridian transports occur when the westerly regime is weak or disrupted and are more frequent during summer (Coudé-Gaussen et al., 1982; Guerzoni et al., 1997; Rodríguez et al., 2001; Torres- Padrón et al., 2002; Ginoux et al., 2004). Three main atmospheric configurations (Fig. 2) favor the transport

of dust from North Africa toward the Mediterranean (Coudé- Gaussen, 1982; Coudé-Gaussen et al., 1987; Bergametti et al., 1989c; Rodríguez et al., 2001): (1) a SW–NE transport (Fig. 2a) toward the northern part of the Mediterranean occurs mostly in winter when a large depression system develops between Canary Islands and the Iberian Peninsula; (2) during interseason, a SE–NW transport (Fig. 2b) is initiated by the simultaneous occurrence of a strong central European anticyclone and of a depression off Portugal; (3) summer dust transport (Fig. 2c) mainly results from the westward shift of the North African anticyclone associated with the remoteness of the Azores high, which provides a SW–NE depression trench along the African coasts toward the Iberian Peninsula and western part of the Mediterranean.

2.4. Clay mineral sources

In order to understand the variations of the clay mineralogy in sediments from the Alboran Sea, the clay mineral assemblages of main source areas were reconstructed using previously published and unpublished data in the frame of the general fluvial, oceanic and atmospheric patterns (Fig. 3). The clay mineralogy of various Mediterranean marine sites has been studied in several marine cores (e.g. Chamley, 1989; Foucault and Mélières, 2000). On average sediments from the western Mediterranean are dominantly composed of 50% illite and 25% kaolinite, with lower amount of smectite (15%) and chlorite (10%) whereas fibrous clays (palygorskite) are present as trace amounts.

Illite generally represents the relative contribution of physical weathering to sedimentation, because this mineral is resistant to degradation and to transport (Chamley, 1989). In the northern Mediterranean (Fig. 3a) the Rhone River and the Po River receiving their detrital material from the Alps are particularly rich in illite associated with some chlorite. As a result, illite dominates the clay mineral association of sediments from the Gulf of Lion (80%) and from the Adriatic Sea (60%) (Tomadin, 2000). Illite is also a major component (35%) of the Ionian Sea sediments (Chamley, 1989) and of the Ebro sedimentary system (35%) (Alonso and Maldonado, 1990). On the North African continent, the relative abundance of illite displays a north–south gradient: illite constitutes 60% of the clay mineral assemblage in northern Algeria, 50% in central Sahara and less than 30% in the Sahelian zone (Paquet et al., 1984). As a result, dust-blown (Fig. 3b) particles originating from Western Sahara are richer in illite (60%) than the particles (30%) issued from central and southern Sahara (Avila et al., 1997).

Kaolinite mainly forms through hydrolysis processes and is typical of highly weathered environment (e.g. Chamley, 1989) such as well-drained lateritic soils characterizing equatorial regions (e.g. Chamley, 1989). Kaolinite (Fig. 3) is thus rare (10%) and reworked from ancient formations in the Rhone and Nile river sediments and even absent in the Po river (e.g. Chamley, 1989), whereas it is much more abundant (30%) in the Ebro river which drains kaolinite rich deposits (Alonso and Maldonado, 1990). In North Africa the distribution of kaolinite depends on the latitude (Paquet et al., 1984): trace amounts in the northern and westernmost part of North Africa, more common in central and South Sahara and abundant in Sahelian and equatorial regions (Pastouret et al., 1978; Caquineau et al., 1998). Moreover kaolinite (Fig. 3b) is more abundant in dust originating from eastern Sahara compare to western Sahara (Guerzoni et al., 1999).

In a general way, smectite is not abundant in the western part of the Mediterranean (Fig. 3a) as a result of the increasing distance from the Nile River, which is the main contributor of smectite in the Mediterranean. The Po and Rhone Rivers do not transport more than 20% of smectite but small Italian coastal and Pyrenean rivers may, respectively, contribute to the supply of smectite in the Tyrrhenian Sea and in the Gulf of Lion (e.g. Chamley, 1989; Foucault and Mélières, 2000). Smectite is rare in the northern Sahara whereas it is abundant in southern Sahara and Sahel. In these areas, smectite may represent 70% of the clay mineral fraction and is associated with kaolinite issued from ancient lateritic profiles (Sarnthein et al., 1982; Paquet et al., 1984; Chamley, 1989). In agreement with this latitudinal distribution, dust originating (Fig. 3b) from western Sahara and Moroccan Atlas are depleted in smectite compared to dust originating from central Algeria and Sahelian sources (Avila et al., 1997).

Although chlorite is often associated with illite, it is far less resistant to weathering and transport. Chlorite thus mainly reflects the composition of nearby source area (Chamley, 1989). In the northwestern part of the Mediterranean basin, the main source of chlorite is the Ebro sedimentary system (35%) (Alonso and Maldonado, 1990) whereas the respective contribution of the Rhone and the Po river is of minor importance (e.g. Chamley, 1989).

Palygorskite is characteristic of the sub-arid belt of the northern hemisphere (Singer and Galan, 1984; Chamley et al., 1989) where its formation is favored by chemically restricted conditions (Singer and Galan, 1984). For instance, evaporation and chemical concentration provide the formation of palygorskite (Fig. 3a) on poorly drained carbonated rocks in the anti-Atlas (El Mouden et al., 2005). But elongated fibers of palygorskite are

usually destroyed during fluvial transport (Chamley, 1989; Snoussi et al., 1990). As a result there are some discrepancies (Fig. 3a) between the composition of the source area and of the mineralogical assemblages recorded in the downstream alluvial sediment (El Mouden et al., 2005). Palygorskite from recent marine deposits off Africa is commonly considered to be dust-blown particles reworked from Neogene North African deposits (e.g. Chamley, 1989). Palygorskite can be distributed through eolian processes over long-range distance as far as Scotland and has been used to trace the Saharan origin of dust (Coudé-Gaussen et al., 1982; Molinaroli, 1996). At present-day, Sahara winds are reported to carry sporadically noticeable amounts of palygorskite over the whole Mediterranean basin (Coudé-Gaussen and Blanc, 1985). For example, some Tunisian loess's are composed of 45% of palygorskite (Grousset et al., 1992). Robert et al. (1984) identified up to 25% of African-derived palygorskite associated to kaolinite in sediments from a high-altitude lake in Corsica (Fig. 3b). Palygorskite represents 10–15% of the clay mineral fraction in northern Algeria (Paquet et al., 1984), 10–25% on the central Algeria and less than 10% in the southern Sahara (Paquet et al., 1984). Similarly, dust from central Algeria and western Sahara (10%) and Morocco Atlas (17%) contain lower amounts of palygorskite than dust deposited (Fig. 3b) in northern Morocco (up to 75%) (Avila et al., 1997).

3. Material and methods

3.1. Stratigraphy

ODP Site 976 (36°12N, 41°8W, 1108m depth) is located in the Alboran Sea, close to the Atlantic–Mediterranean gateway (Fig. 1). Chronology is first based on 17 AMS14C ages (Combourieu Nebout et al., 2002), and then on a correlation between the oxygen isotopes record of site 976 and core MD95-2042 (Cacho et al., 2000) and secondly on correlation between the pollen temperate records of site 976 and $\delta^{18}O$ of ice from the NorthGRIP ice core (NorthGRIP members, 2004). This age scale does not enable us to estimate precisely the vegetation response time compared with the ice-core record, occurring within a few decades to centuries (Masson-Delmotte et al., 2005). Here, we present the uppermost 25m that span a time interval corresponding to the last 50,000 yr.

3.2. Clay mineralogy

All samples were first decalcified with 0.2N hydrochloric acid. The excess acid was removed by H2O washing and repeated centrifugations. The clay-sized fraction (o2mm) was isolated by settling, and oriented on glass slides (oriented mounts). Three X-ray diffraction (XRD) determinations were performed: (a) untreated sample; (b) glycolated sample (after saturation for 12 h in ethylene glycol); (c) sample heated at 49°C for 2 h. The analyses were run on a Philips PW 1710 X-ray diffractometer between 2.49 and 32.51°2theta Each clay mineral is then characterized by its layer plus interlayer interval as revealed by XRD analysis. Smectite is characterized by a peak at 14Å on the untreated sample test, which expands to 17Å after saturation in ethylene glycol and retracts to 10Å after heating. Illite presents a basal peak at 10Å on the three tests (natural, glycolated and heated). Chlorite is characterized by peaks at 14, 7, 4.72 and 3.53Å on the three tests. Kaolinite is characterized by peaks at 7 and 3.57Å on the untreated sample and after saturation in ethylene glycol. Both peaks disappear or are strongly reduced after heating. Palygorskite presents a basal peak at 10.34Å accompanied by a weaker peak at 6.44Å, on both untreated and glycolated tests. The 10.34Å peak collapses at 10Å after heating (Brindley and Brown, 1980). The presence of palygorskite has been confirmed by MET observations of the palygorskite-rich samples. Semi-quantitative estimation of clay mineral abundances, based on the pseudo-Voigt deconvolution for the doublets illite–palygorskite (10–10.34Å) and kaolinite–chlorite (3.57–3.53Å), was performed using the software MacDiff developed by Petschick (2000).

3.3. Pollen analyses and quantitative climate reconstruction

Micropaleontological analyses were performed on the size fraction o125mm, and more than 300 specimens were counted per sample. Pollen methodology follows a classic protocol already developed by Combourieu Nebout et al. (2002). More than a hundred pollen, excluding *Pinus* were counted per sample for paleoenvironmental interpretation. Paleoenvironmental interpretation of the downcore pollen assemblage fluctuations is based on the assumption that the primary pollen contribution to Alboran Sea sediments comes from western Mediterranean borderlands. Modern environments range from a thermo-Mediterranean belt with *Olea*, *Pistacia* and some steppe or semi-desert representatives (*Artemisia*, *Ephedra*), to a meso-Mediterranean belt, represented by a sclerophyllous oak forest to a humid-temperate oak forest (mainly *Quercus* associated with *Ericaceae*), to a supra-Mediterranean belt, with a cold-temperate coniferous forest (*Pinus*, *Abies, Cedrus*) at the higher altitudes (Ozenda, 1975; Rivas-Martinez, 1982).

Around 120 pollen taxa were identified ranging from semi-desert to mountain deciduous and coniferous forest. Their interpretation follows the modern climatic-plant relationships in Eurasia and northern Africa (e.g. Peyron et al., 1998). Here we present the variations of pollen percentages of two main associations: (1) the temperate association composed of European-Siberian trees such as *Quercus, Fagus, CarPinus, Corylus, Alnus, Betula, Tilia and Ulmus* associated with *Ericaceae*, reflecting the warmer and moist climate characteristics of interstadials, and (2) the steppe to semi-desert association, composed of *Artemisia* and *Ephedra*, which marks the dry and cold climatic conditions of the stadials. The analog technique has been applied to the ODP 976 fossil pollen assemblages to provide quantitative estimates of temperatures and precipitation during the last 50,000 yr BP (Guiot, 1990). First developed for continental pollen sequences, the MAT has been tested with success to marine pollen cores from the Mediterranean region (Desprat et al., 2005). In this method, similarity between fossil and modern pollen assemblages is evaluated by a chord distance calculated as a μm of differences between log-transformed percentages of the taxa. Such method does not imply a direct analogy between modern and fossil assemblages, although the quality of the results depends on the size and diversification of the modern data set (Peyron et al., 1998). Here, this technique is based on a modern pollen database including 1510 modern pollen spectra mainly located in the Mediterranean basin (especially Spain and Morocco), Europe and Eurasia (Peyron et al., 1998). Since *Pinus* is overrepresented in marine sediments, this pollen type has been removed from the marine pollen counting as well as from the continental pollen database. The 10 modern spectra which have the smallest chord distance are considered as the best modern analogs of the given pollen spectrum, and used for the reconstruction. The climatic parameters of the 10 best modern analogs are averaged by a weighting inverse to the chord distance. Here, the climatic parameters reconstructed are the mean temperature of the coldest month (°C) and annual precipitation (mm/yr). The error is computed as lower and upper limits of positive and negative deviation of extreme analogs compared to the mean value.

4. Results

4.1. Clay minerals

The average composition of the clay mineral fraction (<2 μm) of the uppermost part of the ODP site 976 (0–25m composite depth), which records the last 50,000 yr, is composed of 33% illite, 31% smectite, 16% kaolinite, 15% chlorite and 5% palygorskite. All clay minerals

show several oscillations during the last glacial period whereas their abundances are less variable during the Holocene (Fig. 4). This apparent weak variability may result from significantly lower sampling resolution within the Holocene (one sample per 500 yr) compared with the last glacial stage (one sample per 300 yr). These results are in good agreement with previous mineralogical studies in the Alboran sea (e.g. Chamley, 1989; Martínez-Ruiz et al., 1999).

Illite represents 28–40% of the total clay mineral fraction. The illite record is characterized by high frequency oscillations of moderate amplitude throughout the core, slightly lower during the Holocene (Fig. 4a). The illite content is maximum around 27 and 22.5 ka (H2) whereas it is minimum around 35 ka, 30 ka (H3), 23.5, 20.5, 18, 13.5, 10 and 7 ka.

The percentages of smectite range between 19% and 42%. The average smectite content decreases slightly between 50 and 22 ka. High-frequency variations are added to this general decreasing trend (Fig. 4b). The relative abundance of smectite is especially low around 38, 32.5, 26 and 20/22 ka (H2), and reaches minimum values around 15 ka (H1). Smectite is abundant around 39, 27.5, 18 and 12 ka reaching maximum values around 36 ka.

The kaolinite record varies between 11% and 24%. The average content of kaolinite increases from last glacial (<15%) to the Holocene (<20%). There is no consistent evolution either during the North Atlantic cold events: an increase of kaolinite is associated with H1 whereas kaolinite is low during H2–H4 (Fig. 4c).

The abundance of chlorite varies between 10% and 22% throughout the core. The chlorite content is higher between 22 and 12 ka than over the rest of the core. High-frequency oscillations overwhelm a slightly increasing trend between 50 and 22 ka. Minimum percentages of chlorite are associated with the HE and with the Younger Dryas (Fig. 4d).

Palygorskite composes 3–11% of the clay mineral fraction. The record is characterized by the presence of several significant peaks, out of the standard deviation range (Fig. 4e). Most of these peaks are associated with cold climatic events, YD and HE (Fig. 4e). H1 and H4 are especially enriched in palygorskite. Except these peaks the record is quite smooth and show very little variations. We can notice a reduce amount of palygorskite during the Holocene.

4.2. Pollen

Palynological records from ODP Site 976 document the classic climatic trend in the Mediterranean region from the glacial times to the Holocene (e.g. Reille and Lowe, 1993; Watts et al., 1996; Allen et al., 1999; Combourieu Nebout et al., 2002; Sánchez-Goñi et al., 2002; Roucoux et al., 2005; Tzedakis, 2005). Variability of pollen assemblages reflects repetitive alternations between temperate forest (mainly *Quercus*), very similar to today's vegetation in the mountains of the western Mediterranean, and semi-desert vegetation as observed today in North African and South- Eastern Europe (Walter et al., 1975) (Fig. 5).

Elevated abundance of temperate pollen taxa occur during warm interstadials, indicating warm and humid climates on continents adjacent to the Alboran sea. Cold stadials correlate with increased *Artemisia* pollen relative abundance that is indicative of enhanced continental aridity (Fig. 5) (Combourieu Nebout et al., 2002). Periods of maximum cooling in the North Atlantic, the HE H1 to H5, are reflected at Site 976 by coeval maxima of semi desert- rich *Artemisia* and minima of *Quercus* forest. Such associations are characteristic of cold steppe to cold desert (Tarasov et al., 1998) and suggest that the western Mediterranean borderlands experienced cold climates and enhanced severe aridity (Combourieu Nebout et al., 2002). These changes in vegetation correlate with modifications in marine environments as revealed by coeval modifications of foraminiferal and dinocysts assemblages that mark cooling of the sea surface temperatures (Combourieu Nebout et al., 2002; Sánchez-Goñi et al., 2002). These episodes were immediately followed by increases of temperate pollen assemblage that document rapid warming and fast increasing humidity in the area.

These results are in agreement with the evidence of higher intensity of wind systems over the northern hemisphere during cold intervals (stadials and HE) revealed by the dust content in Greenland ice cores and other results on continents adjacent to the Alboran sea (Mayewski et al., 1997; Sánchez-Goñi et al., 2002; Moreno et al., 2005).

Climatic parameters reconstructed from pollen analyses reveal repetitive oscillations of mean annual precipitation and mean temperature of the coldest month. During the HE, the pollen-based climatic estimates indicates a decrease of at least 200–400mm in mean annual precipitation and of 5–15°C in mean temperature of the coldest month. The decrease in precipitation is consistent with the elevated abundance of semi-desert taxa. By contrast the reconstructed temperature may appear surprisingly low considering the dominance of *Artemisia* pollen. At present day, the local species *Artemisia* herba–alba is usually associated with MTCO of 0–4°C. More generally, *Artemisia* is today a major component of steppe ad desert environments. Nevertheless, as pollen grains do not permit the determination at species

level, it remains difficult to separate hot and warm steppe or desert in the database because of similar associations. This may induce an accentuation of cold temperatures in our samples, but our results remain generally in accordance with other data in marine and continental records (Allen et al., 1999; Sánchez-Goñi et al., 2002). The database is periodically amended in order to solve this problem and better discriminate these two biomes.

When compared to pollen data the variations of some clay minerals appear to vary together with those of temperate, altitudinal and semi-desert groups (Fig. 5). The variations of palygorskite are positively correlated to semi-arid pollen abundances. As a result, palygorskite and precipitation records exhibit a negative correlation index (-0.41). Although their correlation index is low (r =0.34) chlorite and altitudinal vegetation are somehow linked to each other. By contrast, the kaolinite record appears to be inversely correlated to semi-arid vegetation (r =-0.40) and to the oxygen isotopic ratio (r =-0.40). Illite and smectite do not show any significant correlation with pollen data. Principal Component Analysis of this data set indicates a dominant factor (>80%) retracing the variations of pollen, palygorskite and $\delta^{18}O$ of ice from the NorthGRIP ice core whereas the second factor (<10%) corresponds to the smectite record.

5. Discussion

5.1. Clay mineral supply

All clay minerals records show oscillations during the last glacial, but the increase of palygorskite specifically characterizes the North Atlantic cold events whereas the proportions of illite, kaolinite and smectite do not show consistent variations during these climatic events.

The illite and chlorite primarily discharged by the Rhone River can be further transported from the Gulf of Lion to the Alboran Sea by the oceanic gyre (Millot, 1999). This current is characterized by important seasonal variations (Albérola and Millot, 2003). It is more active during winter than in summer when stratification prevents any convective activity (Durrieu de Madron et al., 1999). The chemical composition and morphology of both illite and chlorite indicate proximal sources from, respectively, Betic Cordilleras and Nevado-Filaboride complexes (Martínez-Ruiz et al., 1999). Similarly morphological analyses of smectite suggest a soil-derived provenance (Martínez-Ruiz et al., 2003). By contrast, the occurrence of elongated fibers of palygorskite within sediments is characteristic of a wind-

421 driven transport. Indeed, there are several evidences that rivers only represent a minor
422 contribution compared to atmosphere at the basin scale (Elbaz-Poulichet et al., 2001),

423 These results indicate that illite, chlorite and smectite are partly transported via rivers
424 toward the Alboran Sea but may also be supplied through eolian processes together with
425 palygorskite. Clay minerals, except palygorskite, are likely to be transported to the Alboran
426 Sea through oceanic, riverine or eolian processes. As a result their variations are less
427 informative than palygorskite ones in terms of global atmospheric configurations.
428 Nevertheless the increase of some of these clay minerals (i.e. illite during H2, kaolinite during
429 H1) or their decrease (i.e. smectite during H3, kaolinite during H2) suggests that regional
430 specific configurations are likely to modify the clay mineral association.

431

432 *5.2. Provenance of palygorskite*

433 The presence of palygorskite (Fig. 4e) and the increase in semi-desert taxa (Fig. 5a
434 and b) characterizing sediments deposited during the cold intervals confirm that arid
435 conditions prevailed on the continent during the North Atlantic cold climatic events (Cacho et
436 al. 2000; Combourieu Nebout et al., 2002; Moreno et al., 2002; Sánchez-Goñi et al., 2002).

437 Because palygorskite is typical of arid and semi-arid climate, it mainly records the
438 North African contribution to sedimentation. Palygorskite is also reported in several
439 formations over the Iberian Peninsula. Although such proximal supply from the Iberian
440 Peninsula has to be taken in account, it is not a major contributor to Alboran deep-sea
441 sedimentation since (1) palygorskite is easily destroyed while transported by rivers and (2)
442 only trace amounts of palygorskite have been detected in proximal sediments. Western
443 Morocco, northern Algeria, central Algeria and southern Sahara (Paquet et al., 1984; El
444 Mouden et al., 2005), as well as reworked Neogene North African deposits (e.g. Chamley,
445 1989), are potential palygorskite source areas.

446 In order to pinpoint its origin, the palygorskite content was compared with the illite-to-
447 kaolinite (I/K) ratio (Fig. 6) which remains unchanged after long-term transport (Caquineau et
448 al., 1998). This comparison gives a rough estimation of the respective contribution of eolian
449 vs. riverine supplies. The I/K ratio (Fig. 6) is also a relevant fingerprint of the regional origin
450 of Saharan dust (Caquineau et al., 1998): dust from North and West Sahara is enriched in
451 illite (I/K =2) whereas kaolinite (I/K =0.1) becomes dominant when the dust has a Sahelian
452 origin (Paquet et al., 1984). South and central Sahara are characterized by intermediate values

(I/K =0.4) (Caquineau et al., 1998). This latitudinal evolution is consistent with the mineralogy of Atlantic sediments and dust collected over the Atlantic Ocean (e.g. Chamley, 1989). The content in kaolinite of dust also varies with the longitude. The I/K ratio decreases from the northwestern Africa (I/K =2–1.1 in northern Algeria) to northeastern Africa (I/K =0.5–0.7) (e.g. Guerzoni and Chester, 1996; Caquineau et al., 1998). In the studied samples the I/K ratio ranges from 1.35 to 3 with an average value of 2.1, and does not significantly change during the old events (Fig. 6). Our data indicate that the eolian contribution should be important in the Alboran Sea since the I/K ratio of proximal riverine supply is rather low (I/ K =1.38) (Alonso and Maldonado, 1990). When compared with data from Caquineau et al. (1998) this ratio suggests sources from the North and West Sahara (I/ K =1.3–2.6) and rules out any contribution from Sahel (I/ Ko0.25) or South and central Sahara (I/K =0.4–0.7). During the North Atlantic cold events, the I/K remains stable while the palygorskite content increases. This result indicates larger contribution of an eolian source characterized by a high palygorskite content and I/K ratio around 2, such as western Morocco (El Mouden et al., 2005). Furthermore, the presence of *Argania* pollen, typical of southern Morocco, associated with the palygorskite within the HE, HE1 and HE4, supports the southern origin of dust. The presence of *Argania* pollen suggests low precipitation (200–400 mm) and positive temperatures. This result is not contradictory with the reconstructed MTCO because this pollen was not used in the MAT modeling and because the occurrence of *Argania* is here interpreted as an evidence of intense eolian transport from southern areas during these HE. *Argania* pollen were probably transported together with palygorskite from southern areas which were not so cold but arid. The sediments from the ODP 976 seem to result from the mixing between riverine supply (possibly the Ebro River) and eolian contributions from North and West Sahara (Fig. 6).

5.3. Palygorskite transport—atmospheric configuration

As palygorskite represents the eolian contribution to deep-sea sedimentation, its abundance suggests that the continental aridity was associated with specific atmospheric configurations favoring dust transport from the source area to the Alboran sea. The different atmospheric scenario leading to palygorskite-rich dust transport issued from Sahara toward Europe are described by specific air-masses trajectories. Several studies (e.g. Avila et al., 1997; Rodríguez et al., 2001), based on decennial observations, attempt to reconstruct the main trajectories of dust outbreaks reaching Europe and their associated atmospheric

configurations (Fig. 7). These dust events are clearly controlled by the intensity of the westerly winds regime over Europe. The migration of both anticyclone and depression cells over the tropical Atlantic, the Mediterranean, the European and North African continents seasonally modulates these situations. According to the potential sources of palygorskite and to the regional wind system, the potential atmospheric configuration resulting in enhanced palygorskite supply during the North Atlantic cold events can then be discussed (Fig. 7).

During summer the thermal convective activity over central and southern Sahara desert lifts dust particles to high atmosphere (Prospero, 1981a, b). This Saharan air mass flows westward at high-altitude. A part of this air mass is further redistributed over long-range distance toward the Mediterranean (pathway 4) by the northern branch of the SAL (Prospero, 1981a, b). This scenario would favor an increased contribution of dust originating from the Lake Chad area. But even if the Bodélé depression is considered to be one of the main dust sources at present-day, there is so far no clear evidence of palygorskite occurrence in dust originating from this area. But few mineralogical studies have attempted to identify fibrous clays so far. The average level of the Lake Chad has dropped during the late Holocene while dustiness increases continuously. These conditions are likely to favor an enhanced production and export of palygorskite toward the Mediterranean if considering Lake Chad as a potential source area. According to our data, there is no significant increase in palygorskite input in the Alboran Sea during the Holocene. The clay mineral fraction composition remains stable over the Holocene. This observation suggests that the Bodélé depression and Lake Chad were probably not the main sources of dust during the North Atlantic cold climatic events.

In the lower trades, below the SAL (850 hPa, 1500 m) the northward transport of desert dust (Fig. 2b) is also seasonally modulated (Bergametti et al., 1989a; Chiapello et al., 1995; Guerzoni et al., 1997; Moulin et al., 1997; Rodríguez et al., 2001). During summer the remoteness of the Azores high and the displacement of the North African anticyclone over Algeria favor the incursion of a depression trench between these two anticyclones gyres (Coudé- Gaussen, 1982; Bergametti et al., 1989a; Moulin et al., 1997; Rodríguez et al., 2001; Torres-Padrón et al., 2002). Dust particles originating from western and central part of the Sahara (Guerzoni et al., 1997) are transported toward the western and central part of the Mediterranean (Figs. 2c and 7, pathway 3) (Moulin et al., 1997). The atmospheric back-trajectories associated with such events indicate that the main dust emission is located in the western part of Morocco, where important source of palygorskite have been identified (Avila

et al., 1997; El Mouden et al., 2005). The increase of palygorskite associated with the North Atlantic cold events could then be tentatively attributed to dominant summer atmospheric configurations. Such meridian circulation of air masses occurs when the westerly regime is weak or disrupted (Coudé-Gaussen, 1982). It would then imply that the North Atlantic cold climatic events are associated with a reduction or a northward shift of the westerlies over Europe. Our results confirm the previous studies in the Alboran sea sediments suggesting a link between the North Atlantic cold events (stadials and HE) and the westerly regime over Europe (Cacho et al., 2000; Combourieu Nebout et al., 2002; Moreno et al., 2002; Sánchez-Goñi et al., 2002)

In winter (Figs. 2b and 7) African dust outbreaks mainly reach Europe through meridian circulation across the Mediterranean (Coudé-Gaussen, 1982). A NS depression trench (Fig. 7) is created between the Azores high (pathway 1) and the high-pressure located over central Mediterranean or over North Africa (Rodríguez et al., 2001; Torres- Padrón et al., 2002). Saharan air masses move northward along the western edge of the high-pressure cell (Coudé- Gaussen, 1982; Rodríguez et al., 2001). The trajectory of such meridian transport is constrained both by the position and the high-pressure cell and the Atlas Mountains (Fig. 7), mainly providing dust and pollen to the northwestern and central Mediterranean. A recent study of southern Europe sedimentary records suggest that this pattern is responsible for the presence of Cedrus pollen originating from northwest Africa and flowering in winter (Magri and Parra, 2002). But the reconstructed trajectories indicate that dust particles were not able to reach the Alboran Sea. This eastern pattern is not likely to influence significantly the sedimentation in the Alboran Sea.

Inter-season Saharan dust outbreaks represent less than 30% of the total dust emission (Guerzoni et al., 1997; Rodríguez et al., 2001). Spring and early summer dust events represent 20% of total annual events (Rodríguez et al., 2001). They are linked to the position of cyclones which favors the air masses crossing the Mediterranean between Tunisia and Egypt toward eastern and central Mediterranean basins (Moulin et al., 1997). Such wind trajectories would not be able to transport fine-dust particles toward the Alboran Sea. At the end of summer the dust main routes are shifted westward because most cyclones originate from the Balearic region. The dust outbreaks have a general NE trajectory toward Corsica and Italy (Bergametti et al., 1989c) (Fig. 7, pathway 1b). Nevertheless the presence of the Atlas mountain (Fig. 7) shift to the East the main direction of dominant winds, preventing any significant contribution to the Alboran Sea sedimentation.

552 Saharan intrusions occurring during fall represent less than 10% of the total annual
553 events (Rodríguez et al., 2001). These events are generally induced by the simultaneous
554 occurrence of a depression off the southwest Iberian Peninsula and of a high-pressure cell
555 over Algeria (Fig. 7, pathway 2) (Rodríguez et al., 2001). The dominant direction of
556 associated winds is likely to transport Saharan dust to the Iberian Peninsula and to the
557 Alboran Sea. Moreover, the dust produced by this synoptic situation probably originates from
558 one of the potential source area of palygorskite (Paquet et al., 1984). But the rare occurrence
559 of such events and their low contribution to the annual dust export suggest they are not the
560 main mechanism leading to palygorskite input in the Alboran Sea. But synoptic situations
561 were different during the last glacial. The enhanced supply associated with the North Atlantic
562 cold events may then indicate that the modern meteorological situation leading to fall Saharan
563 intrusions was much more frequent than today.

564 In summary, according to the provenance of palygorskite and to the atmospheric back-
565 trajectories, the pathways 2 and 3 are the most probable patterns followed by western
566 Moroccan dust-blown particles which characterize the North Atlantic cold events.

567

568 *5.4. Paleoclimatic implications*

569 Glacial periods are characterized by dust fluxes 1.5 to 6 times higher than today
570 especially in tropical oceans (Kolla et al., 1979; Chamley et al., 1989; Ruddiman, 1997;
571 Hoogakker et al., 2004). This enhanced supply was attributed to an aridification of the
572 continents (Kolla et al., 1979; Rea, 1994) and/or to strengthening of the winds (Ruddiman,
573 1997). During glacial intervals, cold and dry conditions develop over the Mediterranean as a
574 result of colder sea surface temperatures associated with the stability of the northern high-
575 pressure cell and with an increased seasonality of precipitations (Prentice et al., 1992; Pérez-
576 Folgado et al., 2003). There is a strong relationship between rainfall and dust storm
577 occurrence (Middleton, 1985). Low precipitations limit the expansion of vegetation, favoring
578 the erosion of unconsolidated fine-grained soil particles (Middleton, 1985; Balsam et al.,
579 1995). As a consequence the aridification is thought to become one of the main factor
580 controlling the production of dust during glacial periods (Kolla et al., 1979; Middleton, 1985;
581 Rea, 1994). But other studies evidenced the influence of wind intensity on the enhanced
582 glacial dust fluxes. Previous studies mainly based on pollen and sediment analyses suggest
583 the intensification of winds, favoring the northward transport of dust across the Mediterranean
584 during the last glacial period. This enhanced eolian input from North Africa was evidenced in

lacustrine sediments from central Italy (Narcisi, 2000) and in terrestrial deposits from a Mediterranean island (Lampedusa) located between Tunisia and Sicily (Giraudi, 2004). The presence of Cedrus pollen, a modern maker of northwest African provenance, in several sites from southern Europe, also supports this hypothesis (Magri and Parra, 2002). Several studies argued that winter transport over the Atlantic ocean should be enhanced during glacial because the most intense present-day dust events originating from the southern Sahelian region typically occur during winter (Chiapello et al., 1997; Ratmeyer et al., 1999; Hoogakker et al., 2004; Washington and Todd, 2005). But major dust outbreaks originating from West and North Sahara also occur during summer (Moulin et al., 1997; Rodríguez et al., 2001; Ginoux et al., 2004). This mechanism should be considered to explain the increased dust fluxes during glacial (Balsam et al., 1995). Grousset et al. (1998) then suggested that both aridity and wind strength should be involved to explain the high glacial dust input. In the frame of the recent studies in the Alboran Sea, our results allow to highlight the importance of eolian processes during the North Atlantic cold events.

In West Mediterranean, cold events as HE and Dansgaard/Oeschger stadials are evidenced by the increase of deep oceanic convection and by the development of arid and cold conditions on the surrounding continents. Locally these cold events seem to be related to changes in atmospheric circulation and intensification of westerly winds (Rohling et al., 1998; Sánchez-Goñi et al., 2002). The increase of steppic plants in Alboran sea sediments associated with low paleoprecipitation estimations indicates that HE were dry and cold (Combourieu Nebout et al., 2002; Sánchez-Goñi et al., 2002). Such a decrease has already been observed in other records in Alboran Sea and off Portugal for HE 3 to 5 (Sánchez-Goñi et al., 2002) and in continental series in Lago Grande di Monticchio, Italy (Allen et al., 1999). It remains slightly higher than the sea surface temperature changes (5–10°C) obtained from alkenones in the Alboran Sea (Cacho et al., 2000) and the temperature of the coldest month deduced from the Monticchio record for the studied period (Allen et al., 1999). As already mentioned in Section 4.2, the small discrepancies between the MTCO at site ODP 976 (Alboran sea) and in Monticchio record may result both from the use of different methods of reconstruction and database. High eolian fluxes based on grain-size measurements, resulting from increased aridity and wind strength, were also evidenced in the Alboran Sea sediments during H3, H4 and H5 (Moreno et al., 2002). Our data also suggest that aridity was enhanced during the North Atlantic cold events, as revealed by steppic vegetation, precipitation estimation and clay minerals (Fig. 5). The presence of palygorskite indicates that peri-Mediterranean areas

were dry with sparse vegetation cover, allowing the erosion of unconsolidated soils. As palygorskite is wind transported, its increase suggests a significant wind strengthening over northern North Africa and allows the reconstruction of the dominant synoptic conditions over the Mediterranean during the North Atlantic cold events. The meridian transport of palygorskite to the Alboran Sea during the North Atlantic cold events implies not only that strong high-pressure cells develop over the tropical Atlantic (Azores High) and over the North African continent (North African High) but also that the westerlies, probably shifted northward, would not prevent the incursion of the Saharan masses toward Europe.

5.5. Relation with the NAO

According to the identification of the main clay sources and to atmospheric back trajectories, the increase of palygorskite during the North Atlantic cold events indicates the stability of two high-pressure cells, the Azores high over the tropical Atlantic Ocean and the North African anticyclone over Algeria. During the North Atlantic cold climatic events, these two high-pressure systems were associated with the existence of a depression over western Europe. The meridian transport of the palygorskite implies that the westerly regime was weak, disrupted or displaced northward. Such synoptic situations are very similar with positive phases of the so-called NAO (Hurrell, 1995). Moulin et al. (1997) evidenced the role of the NAO in controlling the desert dust transport. The NAO is responsible for much of the climate variability observed in the Mediterranean region (Fig. 8) at present-day and possibly during the last glacial (Cacho et al., 2000; Combourieu Nebout et al., 2002; Moreno et al., 2002; Sánchez-Goñi et al., 2002). During positive phase of the NAO, the high-pressure gradient between the strong Azores anticyclone and the Icelandic depression results in a northward shift and an increase strength of the westerlies (Hurrell, 1995). When the NAO is high, dry conditions develop over southern Europe and North Africa (Pittalwala and Hameed, 1991) and the northeast trade winds intensity increases, leading to the enhanced westward transport of desert dust (Moulin et al., 1997). As a result, severe decennial time-scale droughts in Sahel are correlated to low surface temperature in the North Atlantic Ocean (Moulin et al., 1997). Conversely, when the NAO is negative, the pressure gradient between the Azores high and the Iceland low decreases (Hurrell, 1995). The westerlies are shifted to the South providing precipitations over the Mediterranean and the North African continent. Negative phases of the NAO thus prevent dust uptake and transport (Moulin et al., 1997). Several studies in the West Mediterranean and in the Alboran Sea highlight the influence of

northwesterly and Saharan winds in the low sea surface temperatures, in high continental aridity, and in the enhanced dust transport associated with the HE and D/ O stadials.

The modification of the northwesterly regime was compared to the present-day NAO (Cacho et al., 2000; Combourieu Nebout et al., 2002; Moreno et al., 2002, 2005; Sánchez-Goñi et al., 2002), but oscillating with a lower frequency than the decennial one (Hurrell, 1995). High NAO index and increased intensity of the northwesterlies were also invoked to explain the active deep-water convection which occurs in the Mediterranean during HE and stadials (Rohling et al., 1998; Cacho et al., 2000). Furthermore, modeling data indicate high correlation between the winter NAO index and the dust emission from the Bodélé region–Lake Chad area. But this model does not take in account the impact of vegetation reduction on the erodability of soils. Moreover, since no palygorskite was reported so far in dust-blown particles from the Bodélé region, this area cannot be considered as the main dust contributor toward the Alboran sea during the North Atlantic cold events. Our results suggest that palygorskite-rich events are favored by specific atmospheric configurations. A depression corridor is created between the Azores high and the North African anticyclone, leading to the transport of dust particles from western Morocco to the Alboran Sea. Such meridian transfer is efficient only if westerlies are weak, disrupted or displaced northward. But recent studies suggest that the northwesterlies were intense during D/O stadials (Rohling et al., 1998; Cacho et al., 2000; Moreno et al., 2002; Sánchez-Goñi et al., 2002). Our data indicate that northwesterlies should be shifted to the North during the North Atlantic cold events in order to allow the intrusion of Saharan air masses toward Europe. This interpretation is not contradictory with previous studies suggesting intensification of the westerly winds, but may explain the singular feature of the amplified aridity signal characterizing the HE compared to other D/O stadials by shifting the westerly winds toward a more northerly position (Combourieu Nebout et al., 2002; Sánchez-Goñi et al., 2002).

6. Conclusions

The Alboran core ODP 976 provides a combined mineralogical and palynological data set that illustrates connection between climatic and atmospheric system on West Mediterranean throughout the last glacial cycle. Our results provide new insights on the atmospheric configuration in the Alboran Sea during last glacial, especially during the North Atlantic cold events.

683 The increase of palygorskite—a typical wind-blown clay mineral—during these cold
684 episodes suggests the intensification of dust events across the Mediterranean during the North
685 Atlantic cold events. The peculiar mineralogical composition of the clay-size fraction
686 evidences western Morocco as a potential source of dust during the North Atlantic cold
687 events. This hypothesis is supported by the abundance of semi-desert taxa and the presence of
688 *Argania* pollen associated with palygorskite. Coeval palygorskite supply and development of
689 the semi-arid vegetation during the North Atlantic cold events suggest severe droughts on
690 peri-Mediterranean areas, as evidenced by estimated annual precipitations. The enhanced
691 Saharan dust export toward the Alboran Sea during the North Atlantic cold events also
692 implies a strengthening of dominant winds. According to the different air mass trajectories
693 resulting from various atmospheric configurations, summer-type dust events are the best
694 candidate to explain the important transport of fine-particles from western Morocco to the
695 Alboran Sea. According to atmospheric models, such a meridian transport (1) results from the
696 development of strong and stable anticyclonic conditions over the tropical Atlantic and North
697 Africa, similar to today's summer meteorological configuration and (2) implies a northward
698 position of the westerly winds during the North Atlantic cold events.

699 The reconstructed synoptic situation over the West Mediterranean during the North
700 Atlantic cold events was compared with meteorological configurations characterizing the
701 NAO. This observation reveals that the prevailing weather regime over North Africa and
702 western Europe during the North Atlantic cold events was very similar to the one described
703 for positive phases of the NAO, suggesting a systematic shift towards a positive NAO
704 situation.

705 Further geochemical analyses will help to estimate the contribution of the Moroccan
706 source versus other sources such as the Bodélé region during the North Atlantic cold events.
707 Moreover high-resolution mineralogical and palynological studies of sediments deposited
708 during the Marine Isotopic Stage 5 and the Holocene in the Alboran sea will give essential
709 informations on the links between North Atlantic climate and Mediterranean weather regimes.

710

711 **Acknowledgments**

712 We thank the Ocean Drilling Program for making the samples available for that study.
713 We acknowledge J.P. Cazet for his efficient technical assistance. French scientists received
714 financial support from CNRS, from Lille 1 University and from French Program National

715 d'Etude de la Dynamique du Climat (PNEDC). We express our gratitude to Aloys Bory for
716 critical reading of the manuscript. The authors thank F. Grousset and D. Magri for their useful
717 critical reviews. This is Laboratoire des Sciences du Climat et l'Environnement contribution
718 no. 2801.

719

720 **References**

721 Albérola, C., Millot, C., 2003. Circulation in the French Mediterranean coastal zone near
722 Marseille: influence of the wind and of the northern current. Continental Shelf Research 23,
723 587–610.

724 Allen, J.R.M., Brandt, U., Brauer, A., Hubberten, H.-W., Huntley, B., Keller, J., Kraml, M.,
725 Mackensen, A., Mingram, J., Negendank, J.F.W., Nowaczyk, N.R., Oberhänsli, H., Watts,
726 W.A., Wulf, S., Zolitschka, B., 1999. Rapid environmental changes in southern Europe
727 during the last glacial period. Nature 400, 740–743.

728 Alonso, B., Maldonado, A., 1990. Late Quaternary sedimentation patterns of the Ebro
729 turbidite systems (northwestern Mediterranean): two styles of deep-sea deposition. Marine
730 Geology 95, 353–377.

731 Avila, A., Queralt-Mitjans, I., Alarcón, M., 1997. Mineralogical composition of African dust
732 delivered by red rains over northeastern Spain. Journal of Geophysical Research 102 (18),
733 21,977–21,996.

734 Balsam, W.L., Otto-Bliesner, B.L., Deaton, B.C., 1995. Modern and last glacial maximum
735 eolian sedimentation patterns in the Atlantic Ocean interpreted from sediment iron oxide
736 content. Paleoceanography 10, 493–507.

737 Bergametti, G., Dutot, A.L., Buat-Menard, P., Losno, R., Remoudaki, E., 1989a. Seasonal
738 variability of the elemental composition of atmospheric aerosol particles over the
739 northwestern Mediterranean. Tellus 41 (B), 353–361.

740 Bergametti, G., Gomes, L., Coudé-Gaussen, G., Rognon, P., Le Coustumer, M.N., 1989b.
741 African dust observed over Canary islands: source-regions identification and transport pattern
742 for some summer situations. Journal of Geophysical Research 94, 14855–14864.

743 Bergametti, G., Gomes, L., Remoudaki, E., Desbois, M., Martin, D., Buat-Menard, P., 1989c.
744 Present transport and deposition patterns of African dusts to the North-Western
745 Mediterranean. In: Leinen, M., Sarnthein, M. (Eds.), Paleoclimatology and Paleometeorology:

746 Modern and Past Patterns of Global Atmospheric Transport. Serie C/ Mathematical and
747 Physical Sciences. Kluwer Academic, Dordrecht, pp. 227–251.

748 Béthoux, J.P., 1980. Mean water flux across sections in the Mediterranean sea, evaluated on
749 the basis of water and salt budgets and of observed salinities. Oceanologica Acta. 3, 79–88.

750 Brindley, G.W., Brown, G., 1980. Crystal Structures of Clay Minerals and their X-ray
751 Identification. Mineralogical Society, London.

752 Brooks, N., Legrand, M., 2000. Dust variability over northern Africa and rainfall in the Sahel.
753 In: McLaren, S.J., Kniveton, D. (Eds.), Linking Climate Change to Land surface Change.
754 Kluwer Academic, Dordrecht, pp. 1–25.

755 Cacho, I., Grimalt, J.O., Sierro, F.J., Shackleton, N., Canals, M., 2000. Evidence for enhanced
756 Mediterranean thermohaline circulation during climatic coolings. Earth and Planetary Science
757 Letters 183, 417–429.

758 Caquineau, S., Gaudichet, A., Gomes, L., Magonthier, M.-C., Chatenet, B., 1998. Saharan
759 dust: clay ratio as a relevant tracer to assess the origin of soil-derived aerosols. Geophysical
760 Research Letters 25, 983–986.

761 Chamley, H., 1989. Clay Sedimentology. Springer, Berlin.

762 Chamley, H., Debrabant, P., Robert, C., Mascle, G., Rehault, J.P. Aprahamian, J., 1989.
763 Mineralogical and geochemical investigations on latest Miocene deposits in the Tyrrhenian
764 sea (ODP Leg 107). In: Kastens, K., Mascle, J., et al., (Eds.), Ocean Drilling Program,
765 Proceedings 107B. US Government Printing Office, pp. 1501–1513.

766 Chiapello, I., Bergametti, G., Gomes, L., Chatenet, B., Dulac, F., Pimenta, J., Santo Suares,
767 E., 1995. An additional low layer transport of Sahelian and Saharan dust transport over the
768 north-eastern tropical Atlantic. Geophysical Research Letters 22, 3191–3194.

769 Chiapello, I., Bergametti, G., Chatenet, B., Bousquet, P., Dulac, F., Santos Suarez, E., 1997.
770 Origins of African dust transported over the north-eastern tropical Atlantic. Journal of
771 Geophysical Research 102 (D12), 13701–13709.

772 Combourieu Nebout, N., Turon, J.L., Zahn, R., Capotondi, L., Londeix, L., Pahnke, K., 2002.
773 Enhanced aridity and atmospheric high-pressure stability over the western Mediterranean
774 during the North Atlantic cold events of the past 50 ky. Geology 30 (10), 863–866.

775 Coudé-Gaussen, 1982. Les poussières éoliennes sahariennes. Mise au point. Revue de
776 Géomorphologie Dynamique 31, 49–69.

777 Coudé-Gaussen and Blanc, M 1985. Présence de grains éolisés de palygorskite dans les
778 poussières actuelles et les sédiments d'origine désertique. Bulletin de la SociétéGéologique de
779 France 8 (1), 571–579.

780 Coudé-Gaussen, G., Hillaire-Marcel, C., Rognon, P., 1982. Origine et évolution pédologique
781 des fractions carbonatées dans les loess des Matmata (Sud-Tunisien) d'après leurs teneurs en
782 13C et 18O. Comptes Rendus de l'Académie des Sciences de Paris 295, 939–942.

783 Coudé-Gaussen, G., Rognon, P., Bergametti, G., Gomes, L., Strauss, B., Le Coustumer, M.N.,
784 1987. Saharan dust on Fuerteventura island (Canaries): chemical and mineralogical
785 characteristics, air mass trajectories, and probable sources. Journal of Geophysical Research
786 92, 9753–9771.

787 Desprat, S., Sánchez-Goñi, M.F., Turon, J.-L., McManus, J., Loutre, M.F., Duprat, J.,
788 Malaizé, B., Peyron, O., Peypouquet, J.-P., 2005. Is vegetation responsible for glacial
789 inception during periods of muted insolation changes? Quaternary Science Reviews 24 (12–
790 13), 1361–1375.

791 Durrieu de Madron, X., Radakovitch, O., Heussner, S., Loÿe-Pilot, M.- D., Monaco, A., 1999.
792 Role of the climatological and current variability on shelf-slope exchanges of particulate
793 matter: evidence from the Rhoˆ ne continental margin (NW Mediterranean). Deep-Sea
794 Research I 46, 1513–1538.

795 El Mouden, A., Bouchaou, L., Snoussi, M., 2005. Constraints on alluvial clay mineral
796 assemblages in semiarid regions. The Souss Wadi Basin (Morocco, Northwestern Africa).
797 Geologica Acta 3 (1), 3–13.

798 Elbaz-Poulichet, F., Guieu, C., Morley, N.H., 2001. A reassessment of trace metal budgets in
799 the western Mediterranean sea. Marine Pollution Bulletin 42 (8), 623–627.

800 Foucault, A., Mélières, F., 2000. Palaeoclimatic cyclicity in central mediterranean Pliocene
801 sediments: the mineralogical signal. Palaeogeography, Palaeoclimatology, Palaeoecology
802 158, 311–323.

803 Gascó, C., Antón, M.P., Pozuelo, M., Meral, J., González, A.M., Papucci, C., Delfanti, R.,
804 2002. Distributions of Pu, Am and Cs in margin sediments from the western Mediterranean
805 (Spanish coast). Journal of Environmental Radioactiviy 59, 75–89.

806 Ginoux, P., Prospero, J.M., Torres, O., Chin, M., 2004. Long-term simulation of global dust
807 distribution with the GOCART model: correlation with North Atlantic Oscillation.
808 Environmental Modelling and Software 19, 113–128.

809 Giraudi, C., 2004. The upper Pleistocene to Holocene sediments on the Mediterranean island
810 of Lampedusa (Italy). Journal of Quaternary Science 19, 537–545.

811 Grousset, F.E., Rognon, P., Coudé-Gaussen, G., Pédemay, P., 1992. Origins of peri-Saharan
812 dust deposits traced by their Nd and Sr isotopic composition. Palaeogeography,
813 Palaeoclimatology, Palaeoecology

814 Grousset, F.E., Parra, M., Bory, A., Martinez, P., Bertrand, P., Shimmield, G., Ellam, R.M.,
815 1998. Saharan wind regimes traced by the Sr–Nd isotopic composition of subtropical Atlantic
816 sediments: last glacial maximum vs. today. Quaternary Science Reviews 17, 385–409.

817 Guerzoni, S., Chester, R., 1996. The Impact of Desert Dust Across the Mediterranean. Kluwer
818 Academic, Dordrecht.

819 Guerzoni, S., Molinaroli, E., Chester, R., 1997. Saharan dust inputs to the western
820 Mediterranean sea: depositional patterns, geochemistry and sedimentological implications.
821 Deep-Sea Research II 44 (3–4), 631–654.

822 Guerzoni, S., Chester, R., Dulac, F., Herut, B., Loÿe-Pilot, M.-D., Measures, C., Migon, C.,
823 Molinaroli, E., Moulin, C., Rossini, P., Saydam, C., Soudine, A., Ziveri, P., 1999. The role of
824 atmospheric deposition in the biogeochemistry of the Mediterranean sea. Progress in
825 Oceanography 44, 147–190.

826 Guiot, J., 1990. Methodology of the last climatic cycle reconstruction in France from pollen
827 data. Palaeogeography, Palaeoclimatology, Palaeoecology 80, 49–69.

828 Hoogakker, B.A.A., Rothwell, R.G., Rohling, E.J., Paterne, M., Stow, D.A.V., Herrle, J.O.,
829 Clayton, T., 2004. Variations in terrigenous dilution in western Mediterranean sea pelagic
830 sediments in response to climate change during the last glacial cycle. Marine Geology 211,
831 21–43.

832 Hurrell, J.W., 1995. Decadal trend in the North Atlantic Oscillation: regional temperatures
833 and precipitations. Science 269, 676–679.

834 Johnsen, S., Clausen, H.B., Dansgaard, W., Fuhrer, K., Gundestrup, M., Hammer, C.U.,
835 Iversen, P., Jouzel, J., Stauffer, B., Steffensen, J.P., 1992. Irregular glacial interstadials
836 recorded in a new Greenland ice core. Nature 359, 311–313.

837 Kolla, V., Biscaye, P.E., Hanley, A.F., 1979. Distribution of quartz in late Quaternary
838 Atlantic sediments in relation to climate. Quaternary Research 11, 261–277.

839 Loye-Pilot, M.-D., Martin, J.-M., Morelli, J., 1986. Influence of Saharan dust on the rainfall
840 acidity and atmospheric input to the Mediterranean. Nature 321, 427–428.

841 Luck, J.M., Ben Othman, D., 2002. Trace element and Pb isotope variability during rainy
842 events in the NW Mediterranean: constraints on anthropogenic and natural sources. Chemical
843 Geology 182, 443–460.

844 Magri, D., Parra, I., 2002. Late Quaternary western Mediterranean pollen records and African
845 winds. Earth and Planetary Science Letters 200, 401–408.

846 Martínez-Ruiz, F., Comas, M.C., Alonso, B., 1999. Mineral associations and geochemical
847 indicators in upper Miocene to Pleistocene sediments in the Alboran basin (ODP leg 161,
848 Sites 976 and 977). In: Zahn, R., Comas, M.C., Klaus, A. (Eds.), Proceedings of the Ocean
849 Drilling Program, Scientific Results. College Station, TX, pp. 21–36.

850 Martínez-Ruiz, F., Paytan, A., Kastner, M., González-Donoso, J.M., Linares, D., Bernasconi,
851 S.M., Jimenez-Espejo, F.J., 2003. A comparative study of the geochemical and mineralogical
852 characteristics of the S1 sapropel in the western and eastern Mediterranean. Palaeogeography,
853 Palaeoclimatology, Palaeoecology 190, 23–37.

854 Masson-Delmotte, V., Landais, A., Combourieu-Nebout, N., von Grafenstein, U., Jouzel, J.,
855 Caillon, N., Chappellaz, J., Dahl-Jensen, D., Johnsen, S., Stenni, B., 2005. Rapid climate
856 variability during warm and cold periods in polar regions and Europe. C.R. Geosciences

857 337, 935–946.

858 Matthewson, A.P., Shimmield, G., Kroon, D., Fallick, A.E., 1995. A 300 kyr high-resolution
859 aridity record of the north African continent. Paleoceanography 10, 677–692.

860 Mayewski, P.A., Meeker, L.D., Twickler, M.S., Whitlow, S., Yang, Q., Lyons, W.B.,
861 Prentice, M., 1997. Major features and forcing of high latitude northern hemisphere
862 atmospheric circulation using a 110,000- year-long glaciochemical series. Journal of
863 Geophysical Research 102, 23,366–26,345.

864 Middleton, N.J., 1985. Effect of drought on dust production in the Sahel. Nature 316, 431–
865 434.

866 Milliman, J.D., Meade, R.H., 1983. World-wide delivery of river sediment to the oceans.
867 Journal of Geology 91, 1–21.

868 Millot, C., 1999. Circulation in the western Mediterranean Sea. Journal of Marine Systems
869 20, 423–442.

870 Molinaroli, E., 1996. Mineralogical characterization of Saharan dust with a view to its final
871 destination in Mediterranean sediments. In: Guerzoni, S., Chester, R. (Eds.), The Impact of
872 Desert Dust across the Mediterranean. Kluwer Academic, Dordrecht, pp. 153–162.

873 Moreno, A., Cacho, I., Canals, M., Prins, M.A., Sánchez-Goñi, M.F., Grimalt, J.O., Weltje,
874 G.J., 2002. Saharan dust transport and high latitude glacial climatic variability: the Alboran
875 sea record. Quaternary Research 58, 318–328.

876 Moreno, A., Cacho, I., Canals, M., Grimalt, J.O., Sánchez-Goñi, M.F., Shackleton, N., Sierro,
877 F.J., 2005. Links between marine and atmospheric processes oscillating on a millennial time-
878 scale. A multiproxy study of the last 50,000 yr from the Alboran sea. Quaternary Science
879 Reviews 24, 1623–1636.

880 Moulin, C., Lambert, C.E., Dulac, F., Dayan, U., 1997. Control of atmospheric export of dust
881 from north Africa by the north Atlantic Oscillation. Nature 387, 691–694.

882 Narcisi, B., 2000. Late Quaternary eolian deposition in central Italy. Quaternary Research 54,
883 246–252.

884 NorthGRIP members, 2004. High resolution climate record of the northern hemisphere back
885 to the last interglacial period. Nature 431, 147–151.

886 Ozenda, P., 1975. Sur les étages de végétation dans les montagnes du bassin Méditerranéen.
887 Documents de Cartographie Ecologique 16, 1–32.

888 Paquet, H., Coudé-Gaussen, G., Rognon, P., 1984. Etude minéralogique de poussières
889 sahariennes le long d'un itinéraire entre 19° et 35° de latitude nord. Revue de Géologie
890 Dynamique et de Géographie Physique 25, 257–265.

891 Pastouret, L., Chamley, H., Delibrias, G., Duplessy, J.C., Thiede, J., 1978. Late Quaternary
892 climatic changes in western tropical Africa deduced from deep-sea sedimentation of the Niger
893 delta. Oceanologica Acta 1 (2), 217–232.

894 Pérez-Folgado, M., Sierro, F.J., Flores, J.A., Cacho, I., Grimalt, J.O.,

895 Zahn, R., Shackleton, N., 2003. Western Mediterranean planktonic foraminifera events and
896 millennial climatic variability during the last 70 kyr. Marine Micropaleontology 48, 49–70.

897 Petschick, 2000. MacDiff Freeware.

898 Peyron, O., Guiot, J., Cheddadi, R., Tarasov, P., Reille, M., de Beaulieu, J.-L., Bottema, S.,
899 Andrieu, V., 1998. Climatic reconstruction in Europe for 18,000 yr BP from pollen data.
900 Quaternary Research 49, 183–196.

901 Pittalwala, I., Hameed, I., 1991. Simulation of the North Atlantic Oscillation in a general
902 circulation model. Geophysical Research Letters 18, 841–844.

903 Prentice, I.C., Cramer, W., Harrison, S.P., Leemans, R., Monserud, R.A., Solomon, A.M.,
904 1992. A global biome model based on plant physiology and dominance, soil properties and
905 climate. Journal of Biogeography 19 (2), 117–134.

906 Prospero, 1981b. Arid regions as sources of minerals aerosols in the marine atmosphere.
907 Geological Society of America, Special paper 186, 71–86.

908 Prospero, 1981b. Eolian transport to the world ocean. In: Emiliani, C. (Ed.), The Sea VII the
909 Oceanic Lithosphere. Wiley, New York, pp. 871–874.

910 Prospero, J.M., Glacuum, R.A., Nees, R.T., 1981. Atmospheric transport of soil dust from
911 Africa to South America. Nature 289, 570–572.

912 Pye, K., 1987. Aeolian Dust and Dust Deposits. Academic Press, San Diego, USA.

913 Ratmeyer, V., Fischer, G., Wefer, G., 1999. Lithogenic particle fluxes and grain-size
914 distributions in the deep ocean off northwest Africa: implications for seasonal changes of
915 aeolian dust input and downward transport. Deep-Sea Research I 46, 1289–1337.

916 Rea, D.K., 1994. The paleoclimatic record provided by eolian deposition in the deep ocean:
917 the geologic history of wind. Reviews of Geophysics 32, 159–195.

918 Rea, D.K., Leinen, M., Jacenek, T.R., 1985. Geologic approach to the long-term history of
919 atmospheric circulation. Science 227, 721–725.

920 Reille, M., Lowe, J.J., 1993. A re-evaluation of the vegetation history of the Eastern Pyrénées
921 (France) from the end of the glacial to the present. Quaternary Science Reviews 12, 47–77.

922 Rivas-Martinez, S., 1982. Etages bioclimatiques, secteurs chronologiques et séries de
923 végétation de l'Espagne méditerranéenne. Ecologia

924 Mediterranea 8, 275–288.

925 Robert, C., Gauthier, A., Chamley, H., 1984. Origine autochtone et allochtone des argiles
926 récentes de haute altitude en Corse. Géologie de la Méditerranée XI, 243–253.

927 Rodríguez, S., Querol, X., Alastuey, A., Kallos, G., Kakaliagou, O., 2001. Saharan dust
928 contributions to PM10 and TSP levels in Southern and Eastern Spain. Atmospheric
929 Environment 35, 2433–2447.

930 Rognon, P., Coudé-Gaussen, G., Revel, M., Grousset, F.E., Pédemay, P., 1996. Holocene
931 Saharan dust deposition on the Cape Verde islands: sedimentological and Nd–Sr isotopic
932 arguments. Sedimentology 43, 359–366.

933 Rohling, E.J., Hayes, A., de Rijk, S., Kroon, D., Zachariasse, J.W., 1998. Abrupt cold spells
934 in the NW Mediterranean. Paleoceanography 13, 316–322.

935 Roucoux, K.H., de Abreu, L., Shackleton, N.J., Tzedakis, P.C., 2005. The response of NW
936 Iberian vegetation to North Atlantic climate oscillations during the last 65 kyr. Quaternary
937 Science Review 24, 1637–1653.

938 Ruddiman, W.F., 1997. Tropical Atlantic terrigenous fluxes since 25,000 yr. Marine Geology
939 136, 18–207.

940 Ruddiman, W.F., Sarnthein, M., Backman, J., Baldauf, J.G., Curry, W., Dupont, L.M.,
941 Janecek, T., Pokras, E.M., Raymo, M., Stabell, B., Stein, R., Tiedemann, R., 1989. Late
942 Miocene to Pleistocene evolution of climate in Africa and the low-latitude Atlantic: overview
943 of leg 108 results. In: Ruddiman, W.F., Sarnthein, M., et al., (Eds.), Proceedings of the Ocean
944 Drilling Program, Scientific Results, pp. 463–484.

945 Sánchez-Goñi, M.F., Cacho, I., Turon, J.L., Guiot, J., Sierro, F.J., Peypouquet, J.-P., Grimalt,
946 J.O., Shackleton, N., 2002. Synchroneity between marine and terrestrial responses to
947 millennial scale climatic variability during the last glacial period in the Mediterranean region.
948 Climate dynamics 19, 95–105.

949 Sarnthein, M., Thiede, J., Pflaumann, U., Erlenkeuser, H., Fütterer, D., Koopmann, B., Lange,
950 H., Seibold, E., 1982. Atmospheric and oceanic circulation patterns off Northwest Africa
951 during the past 25 million years. In: Rad, U., Hinz, K., Sarnthein, M., Seibold, E. (Eds.),
952 Geology of the Northwest African Continental Margin. Springer, Berlin, pp. 545–604.

953 Schütz, L., 1980. Long-range transport of desert dust with special emphasis on the Sahara.
954 Annual of the New York Academy of Science 338, 515–532.

955 Singer, A., Galan, E., 1984. Palygorskite–Sepiolite. Occurences, Genesis and Uses.
956 Developments in Sedimentology. Elsevier, Amsterdam.

957 Snoussi, M., Jouanneau, J.M., Latouche, C., 1990. Flux de matières issues des bassins
958 versants de zones semi-arides (bassin du Sebou et du Souss, Maroc). Importance dans le bilan
959 global des apports d'origine continentale parvenant à l'océan mondial. Journal of African
960 Earth Sciences 11 (1–2), 43–54.

961 Stanley, D.J., Warne, A.G., Davis, H.R., Bernasconi, S.M., Chen, Z., 1992. Nile delta.
962 National Geographic Research Exploration 8 (1), 22–51.

963 Tarasov, P.E., Cheddadi, R., Guiot, J., Bottema, S., Peyron, O., Belmonte, J., Ruiz-Sanchez,
964 V., Saasi, F., Brewer, S., 1998. A method to determine warm and cool steppe biomes from
965 pollen data: application to the Mediterranean and Kazakhstan regions. Journal of Quaternary
966 Science 13, 335–344.

967 Tomadin, L., 2000. Sedimentary fluxes and different dispersion mechanisms of the clay
968 sediments in the Adriatic basin. Rendiconti Scienze Fisiche e Naturali Accademia Lincei 9
969 (11), 161–174.

970 Tomadin, L., Lenaz, R., 1989. Eolian dust over the Mediterranean and their contribution to
971 the present sedimentation. In: Leinen, M., Sarnthein, M. (Eds.), Paleoclimatology and
972 Paleometeorology: Modern and Past Patterns of Global Atmospheric Transport. Series C/
973 Mathematical and Physical Sciences. Kluwer academic, Dordrecht, pp. 267–281.

974 Torres-Padrón, M.E., Gelado-Caballero, M.D., Collado-Sánchez, C., Siruela-Matos, V.F.,
975 Cardona-Castellano, P.J., Hernández-Brito, J.J., 2002. Variability of dust inputs to the
976 CANIGO zone. Deep-Sea Research II 49, 3455–3464.

977 Tzedakis, P.C., 2005. Towards an understanding of the response of southern European
978 vegetation to orbital and suborbital climate variability. Quaternary Science Reviews 24,
979 1585–1599.

980 Walter, W., Harnickell, E., Mueller-Dombois, D., 1975. Climate-Diagram Maps. Springer,
981 Berlin.

982 Washington, R., Todd, M.C., 2005. Atmospheric controls on mineral dust emission from the
983 BodéléDepression, Chad: the role of the low level jet. Geophysical Research Letters 32
984 (L17701).

985 Watts, W.A., Allen, J.R.M., Huntley, B., 1996. Vegetation history and palaeoclimate of the
986 last glacial period at Lago Grande di Monticchio, southern Italy. Quaternary Science Reviews
987 15, 133–153.

988

989

990 **Figure captions**

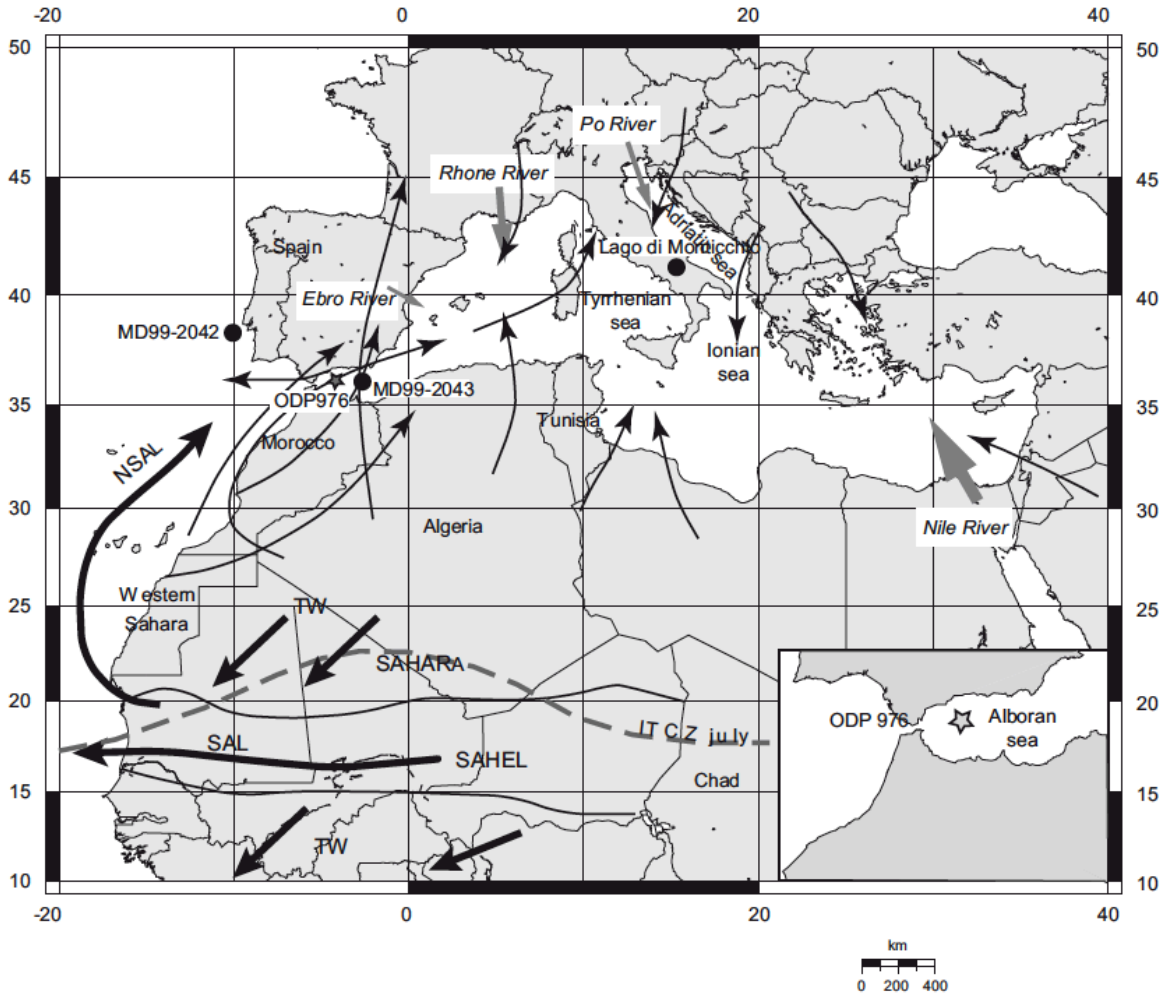

991

992 Fig. 1. Geographical settings. Main wind trajectories (black arrow) and rivers supply (gray
993 arrow) in the Mediterranean area. The geographical boundary between Sahara and Sahel is
994 reported. SAL: Saharan air layer, TW: northeast trade winds, NSAL: northern branch of the
995 SAL, ITCZ July: position of the Inter-Tropical Convergence Zone in July.

996

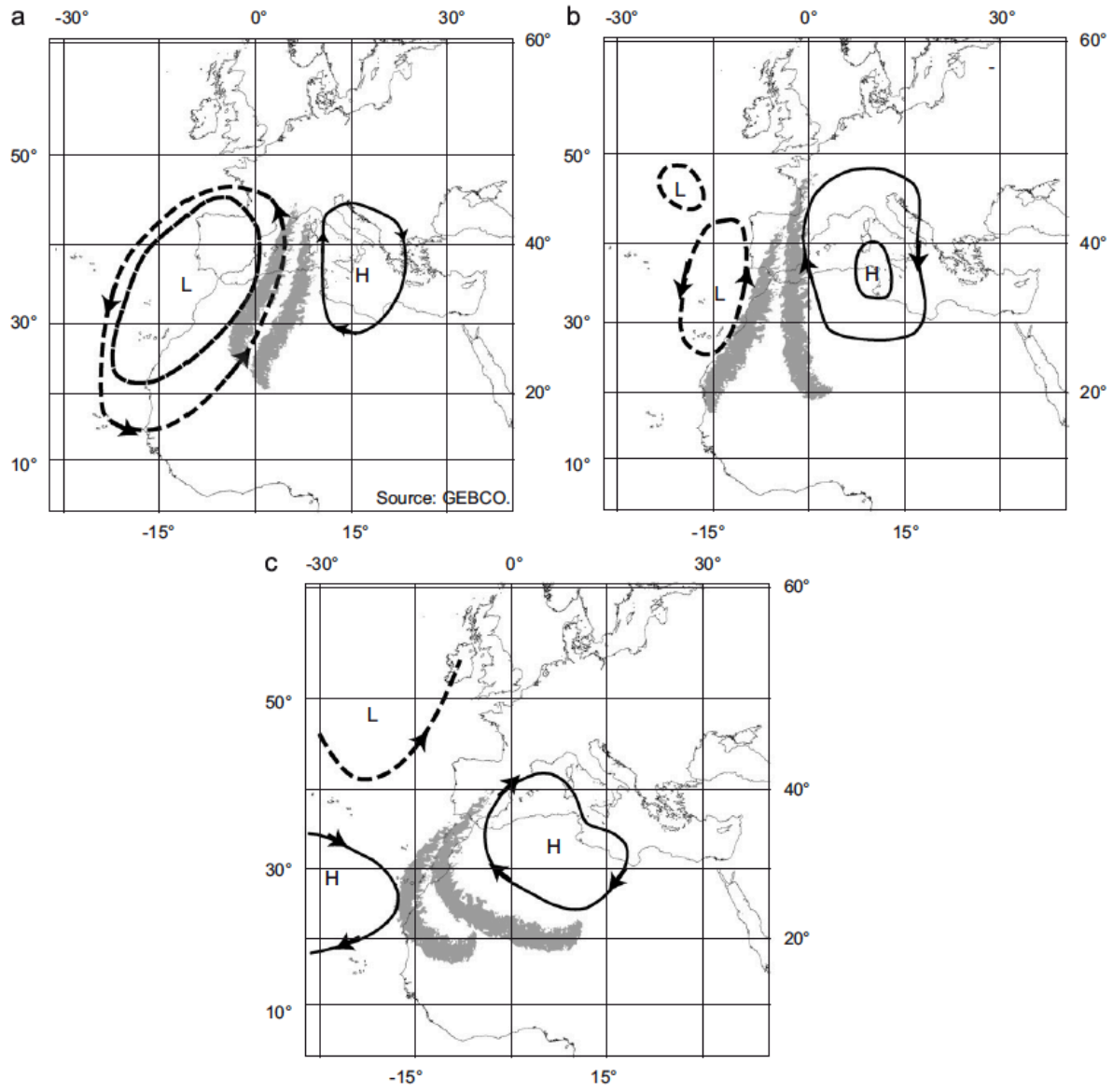

997

998 Fig. 2. Three main atmospheric configurations favouring the meridian transport of Saharan
999 dust toward Europe during winter (a) strong low pressure (L) over the Iberian peninsula,
1000 during fall (b) strong high pressure (H) over central Mediterranean combined with a low
1001 pressure off Portugal, and during summer (c) strong low pressure over North Africa and
1002 tropical Atlantic and low pressure over North Atlantic. Modified from (Coudé-Gaussen, 1982;
1003 Rodríguez et al., 2001).

1004

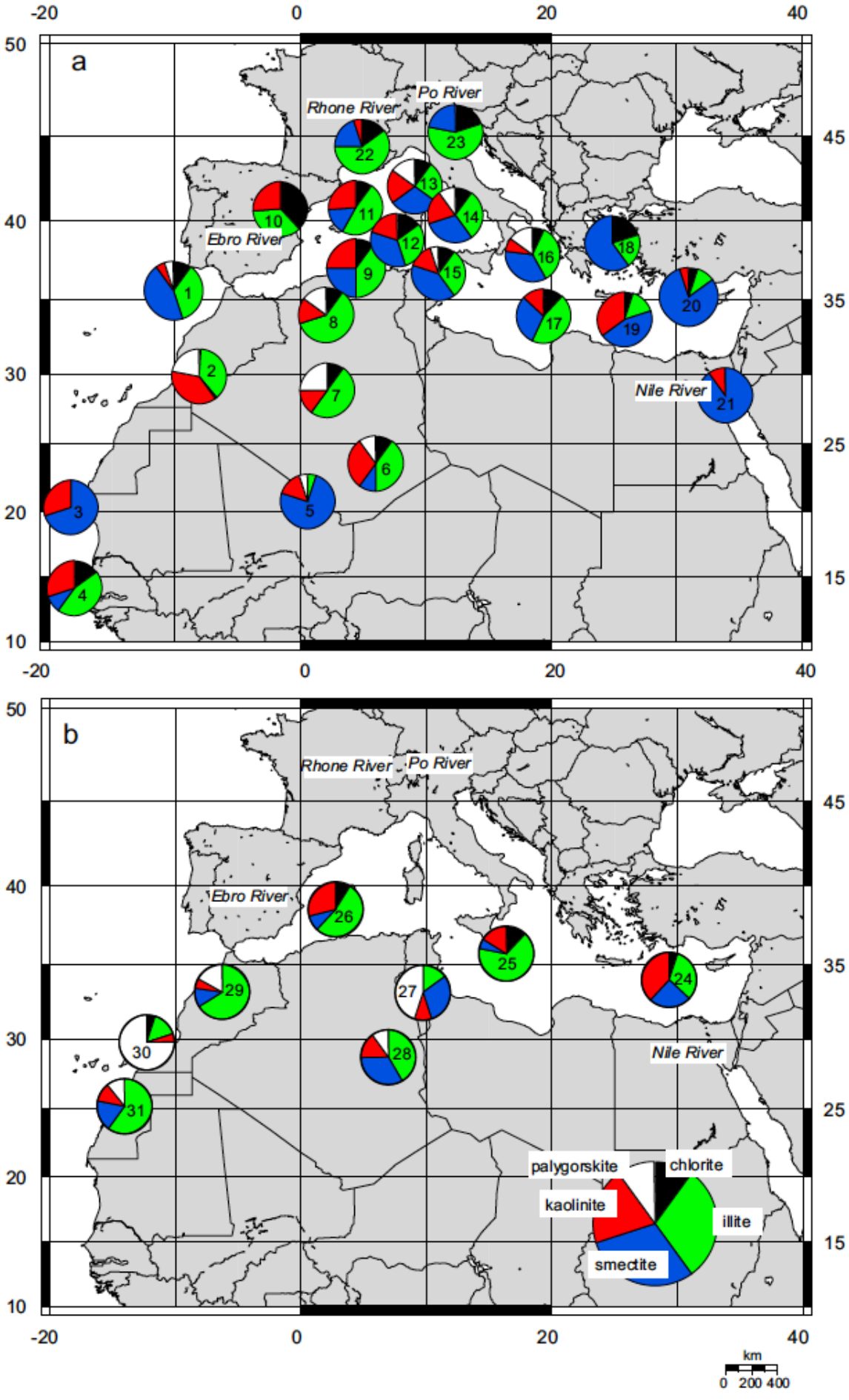
a
Rhone River
Po River
Ebro River
Nile River
b
Rhone River
Po River
Ebro River
Nile River
palygorskite
chlorite
kaolinite
illite
smectite
km
0 200 400

Fig. 3. Clay mineralogy of (a) peri-Mediterranean river particles and sediments (in %) and (b) dust and aerosols (Pastouret et al., 1978; Coudé-Gaussen, 1982; Paquet et al., 1984; Robert et al., 1984; Chamley, 1989; Alonso and Maldonado, 1990; Grousset et al., 1992; Avila et al., 1997; Guerzoni et al., 1999; El Mouden et al., 2005). 1: Gibraltar, 2: Morocco; 3: Cape blanc, 4: Cape Verde, 5: Tanezrouft, 6: Tamanrasset, 7: In Salah, 8: northern Algeria, 9: Algerian shelf, 10: Ebro river, 11: western Mediterranean sediments, 12: Sardinia, 13: Corsica, 14: Tyrrhenian sea, 15: Malta, 16: Ionian sea, 17: central Mediterranean sediments, 18: eastern Mediterranean sediments, 19: Aegean sea, 20: Florence rise, 21: Nile river, 22: Rhone river, 23: Po river, 24 eastern Mediterranean aerosols, 25: central Mediterranean aerosols, 26: western Mediterranean aerosols, 27: Tunisian loess, 28: dust from central Algeria, 29: dust from Moroccan Atlas, 30: Moroccan dust, 31: dust from central Sahara.

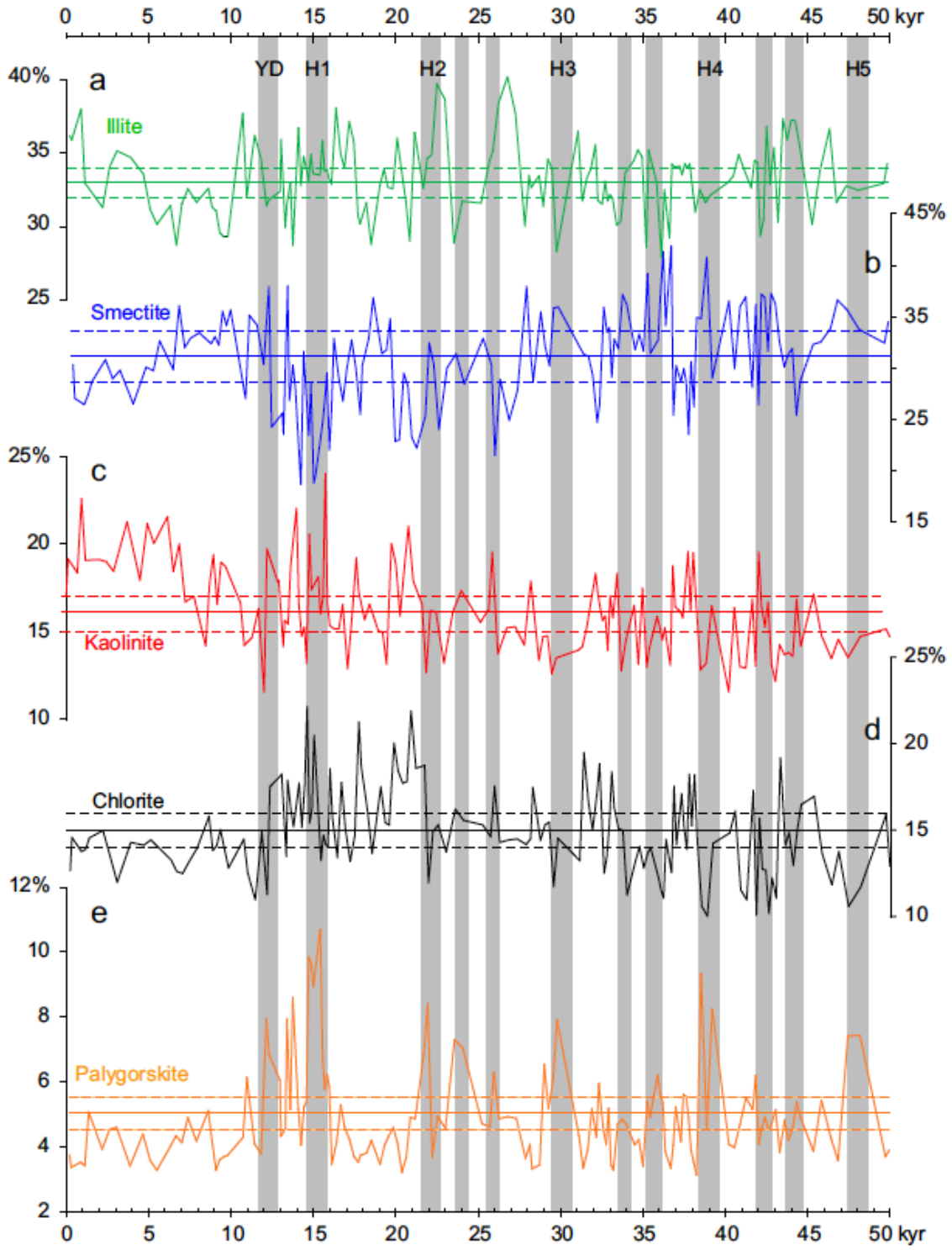

1018

1019 Fig. 4. Clay minerals variations (%) with time (ka): (a) illite, (b) smectite, (c) kaolinite, (d)
1020 chlorite and (e) palygorskite. Time-slices corresponding to the Younger Dryas (YD) and to
1021 Heinrich events 1 to 5 (H1 to H5) are delimited by gray rectangle.

1022

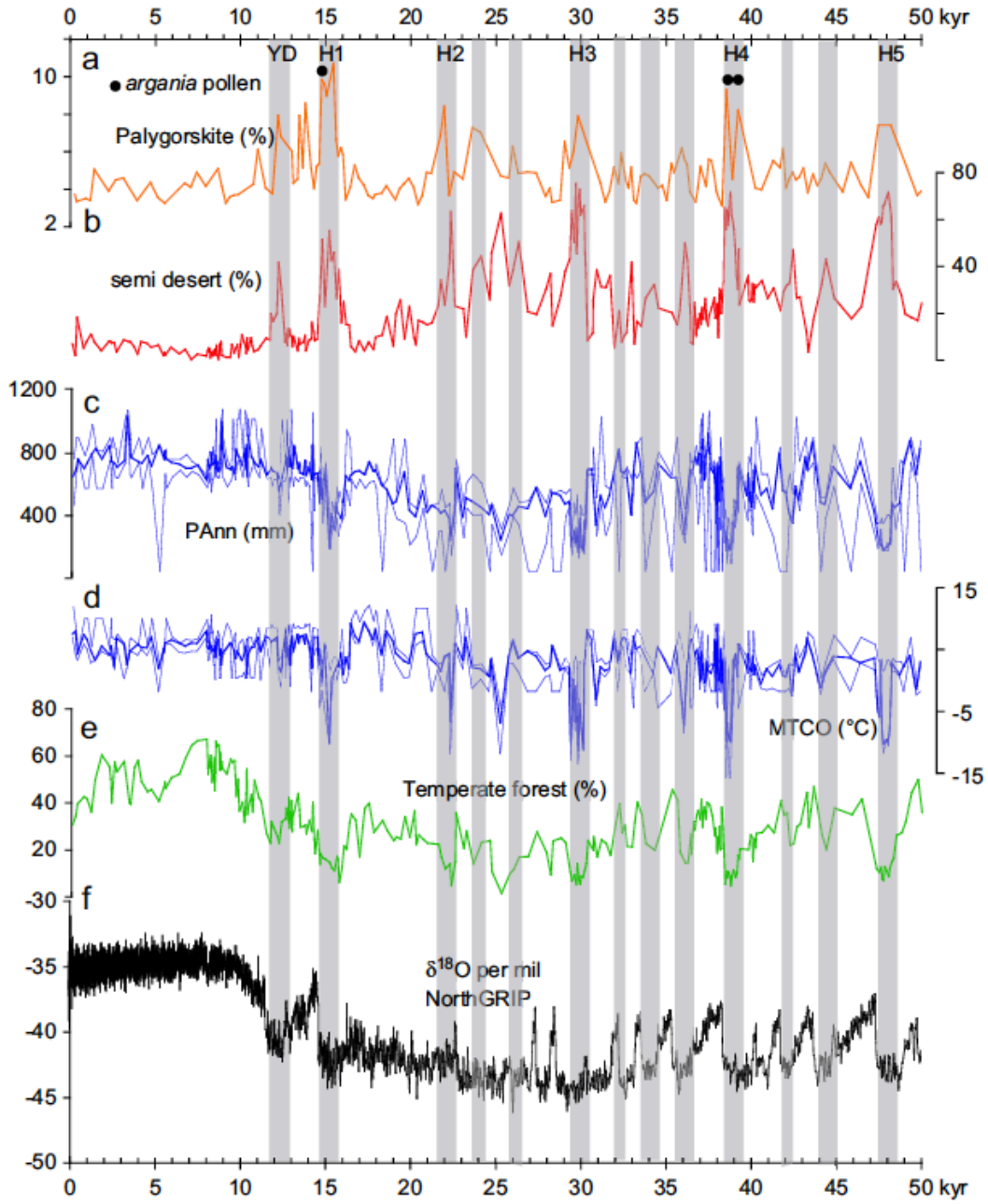

1023

1024 Fig. 5. (a) Palygorskite content (%), (b) semi-desert vegetation abundance (%), (c) annual
1025 precipitation (Pann in mm) and (d) mean temperature of the coldest month (MTCO) based on
1026 the modern analog technique (see text for explanation) with sigma errors, (e) temperate pollen
1027 (%) and (f) oxygen isotopic ratio at NorthGRIP (%). Time-slices corresponding to the
1028 Younger Dryas (YD) and to Heinrich events 1 to 5 (H1 to H5) are delimited by gray
1029 rectangle. A black circle marks the presence of *Argania* pollen.

1030

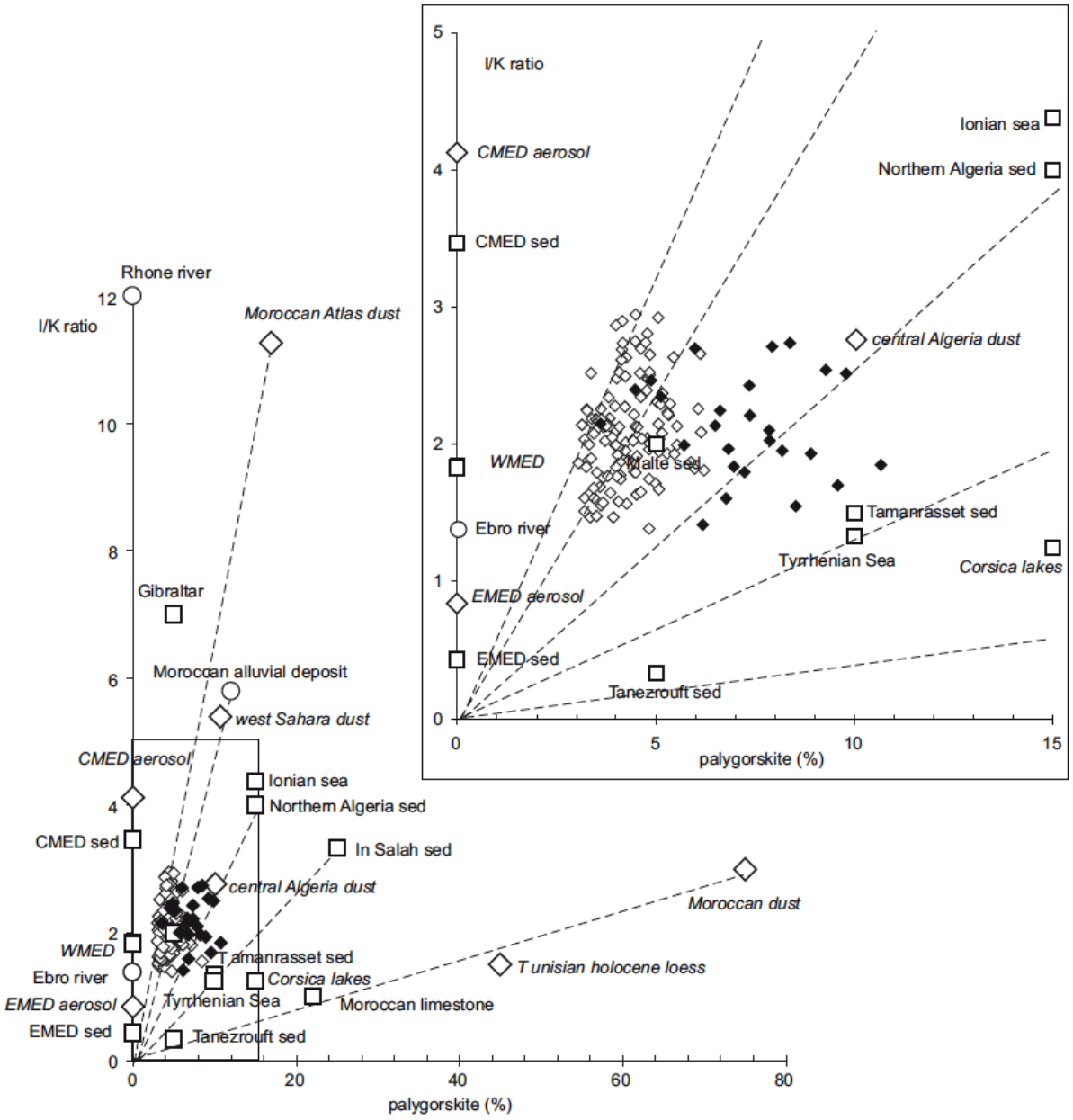

1031

1032 Fig. 6. (a) Palygorskite content (%) versus illite-to-kaolinite ratio (I/K) of ODP 976 sediments
1033 (diamonds) and of main end-members: rivers (circle), dust and aerosols (star), and sediments
1034 (square). Black diamonds correspond to Younger Dryas and Heinrich events samples. Mixing
1035 lines between end members are suggested (dotted lines), (b) enlarged view of (a). CMED:
1036 central Mediterranean, EMED: eastern Mediterranean, WMED: western Mediterranean.

1037

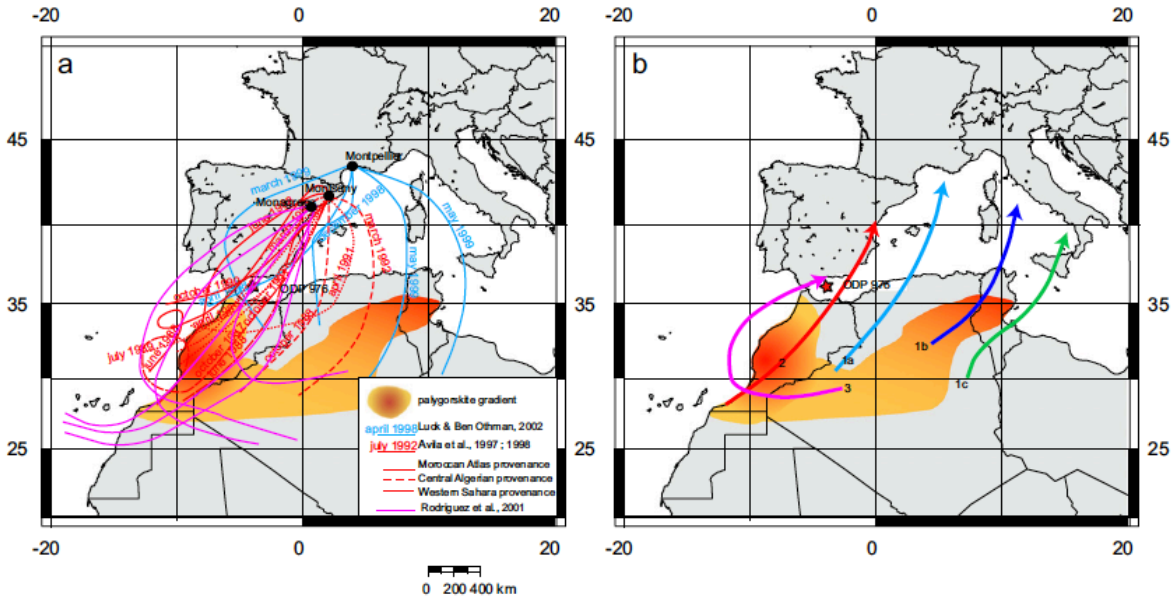

1038

1039 Fig. 7. Main potential sources of palygorskite with gradient ranging from >25% (dark orange)
1040 to 10% (light orange) and (a) main air masses trajectories for different dust events ending at
1041 Montpellier, France (blue lines), Montseny station, Spain (red lines), and Monanegra station,
1042 Spain (pink lines) with respect to their respective origin: thin dotted-line for Moroccan Atlas
1043 provenance; medium dotted-line for central Algeria provenance and thick dotted-line for
1044 western Sahara provenance (Avila et al., 1997; Rodríguez et al., 2001; Luck and Ben Othman,
1045 2002), (b) main average dust trajectories reaching Europe.

1046

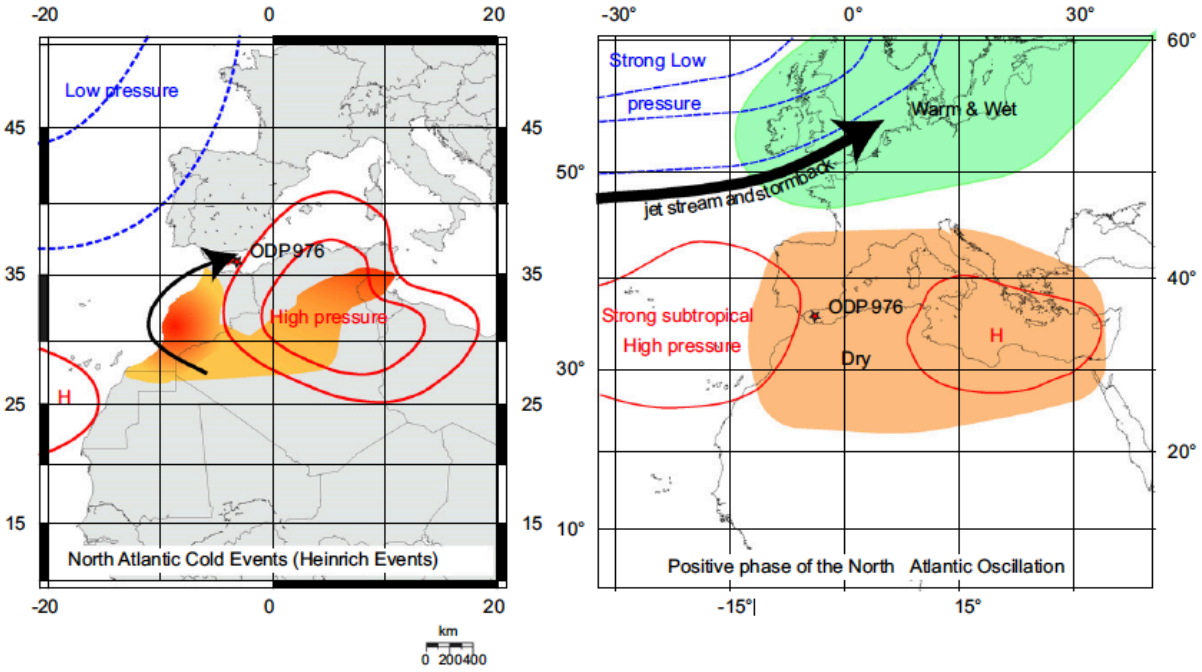

1047

1048 Fig. 8. Synoptic atmospheric configurations over the Mediterranean and the North Atlantic
1049 Ocean (a) during the north Atlantic cold events and (b) associated with positive phase of the
1050 North Atlantic Oscillation (Hurrell, 1995).